BYG·DTU

João Luís Domingues Costa

Standard Methods for Seismic Analyses

DANMARKS
TEKNISKE
UNIVERSITET

Report
BYG·DTU
R-064
2003
ISSN 1601-2917
ISBN 87-7877-129-9

João Luís Domingues Costa

Standard Methods for Seismic Analyses

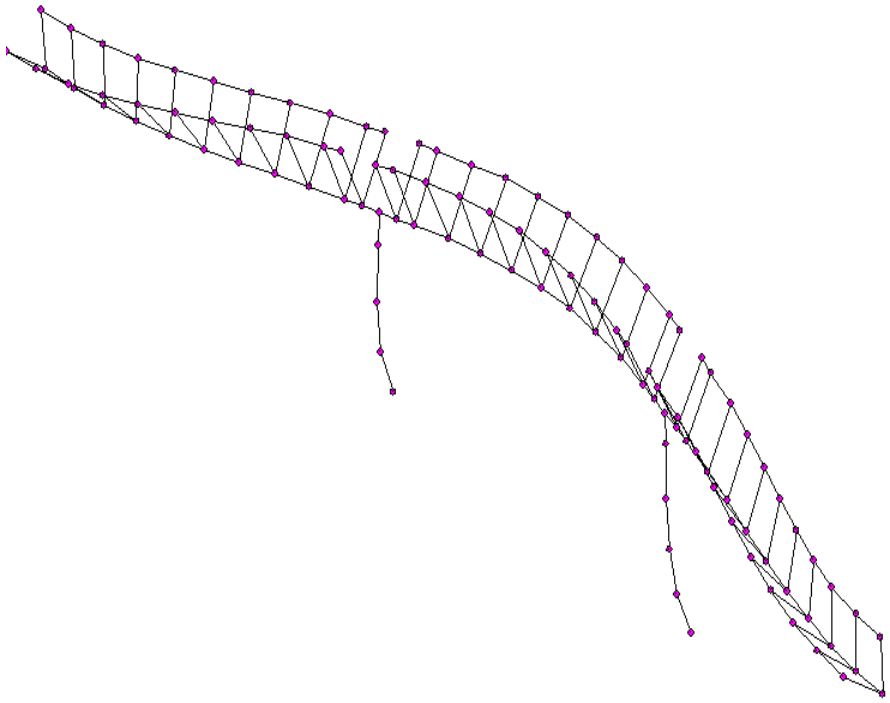

Report
BYG · DTU R-064
2003
ISSN 1601-2917
ISBN 87-7877-126-9

Contents

Acknowledgements

The work has been carried out at the Department of Structural Engineering and Materials, Technical University of Denmark (BYG • DTU) under the supervision of Professor, Dr. techn. M. P. Nielsen.

The author would like to thank his supervisor for giving valuable advice and inspiration as well as valuable criticism to the present work.

Thanks are also due to the author's co-supervisor M.Sc. Ph.D. Rita Bento, Instituto Superior Técnico, Lisbon, Portugal, who has given important and useful comments and suggestions.

A word of appreciation should also be addressed to Civil Engineer Ph D Junying Liu, COWI A/S, for providing the example used in the case study and for assistance in carrying out the study.

The Portuguese institution for scientific research Fundação para a Ciência e Tecnologia – FCT, sponsors the Ph.D. project under which this report was done. The author grateful acknowledges this support.

Lyngby, July 2003

João Luís Domingues Costa

1. Introduction

The following report gives a general survey of the most important methods nowadays at disposal for a structural engineer when performing a seismic design of a given structure.

The methods to be discussed are the response spectrum method and the linear time--history analysis. The first one is widely used as it applies to the major part of a seismic analysis necessary for design purpose. The time-history response method provides more detailed information regarding the seismic behaviour of a structure and is therefore used for more specific earthquake analyses. Both methods assume linear behaviour of the structure, i.e. proportionality between deformations and forces. For its simplicity, the static equivalent method, usually used in the pre-design phase of regular structures, is also introduced.

The theoretical information given in this report is complemented with analysis of a bridge similar to one designed for the High Speed Transportation System in Taiwan.

This document is intended for students or civil engineers who want to have a basic knowledge about earthquake analysis. Before discussing seismic analysis in particular, the reader is introduced to some of the corresponding basic concepts from elementary Structural Dynamics.

It should be noted that this report does not intend to be neither a reference book nor a Structural Dynamics or Earthquake Analysis textbook. For further study a number of references are given.

2. Structural Dynamics Fundamentals

2.1 Formulation of Equation of Motion for SDOF Systems

The essential properties of any linearly elastic structural system subjected to dynamical loads include its mass, *m*, its elastic characteristics (stiffness), *k*, and its energy loss mechanism (damping), characterized by a number *c*. In dynamical terms, a system is called a Single Degree of Freedom (SDOF) system if all these properties may be modelled by a physical element with only one component of displacement, *q*. See figure 1 a).

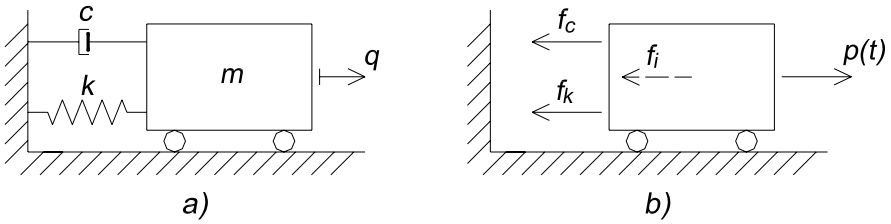

Figure 1 – a) Simplified sketch of a SDOF system; b) Dynamical equilibrium of a SDOF system

The primary objective in a structural dynamical analysis is to evaluate the time variation of the displacements and to accomplish this the *Equation of Motion* must be formulated and solved.

One of the methods to formulate the Equation of Motion[1] is direct use of Newton's second law, which implies that the mass develops an inertia force, f_i, proportional to its acceleration and opposing the acceleration. The dynamical equilibrium condition is given by (2.1)[2].

$$\begin{aligned} F(t) - f_i(t) = 0 \Leftrightarrow \\ \Leftrightarrow F(t) - m \cdot \ddot{q}(t) = 0 \end{aligned} \tag{2.1}$$

Referring to Figure 1 b) the resultant force acting on the mass, *F(t)*, may be defined as the difference between the external loads *p(t)* and the sum of the elastic forces, f_k, and the damping forces, f_c. The equilibrium condition may then be written as follows:

$$f_i + f_c + f_k = p(t) \tag{2.2}$$

- Elastic forces, f_k, are determined using Hooke's law:

$$f_k = k \cdot q(t) \tag{2.3}$$

[1] Chapter 1-5 and chapter 2-2 of reference 1 on the formulation of the Equation of Motion is recommended.

[2] A dot means differentiation with respect to time

- Damping forces, f_c, of the viscous type are proportional to the velocity, i.e.[3].

$$f_c = c \cdot \dot{q}(t) \tag{2.4}$$

Introducing equations (2.3) and (2.4) into equation (2.2) one may write the equilibrium condition in terms of the coordinate *q(t)*, the system properties, *m*, *k* and *c* and the external dynamical loads as follows:

$$m \cdot \ddot{q}(t) + c \cdot \dot{q}(t) + k \cdot q(t) = p(t) \tag{2.5}$$

This last expression is known as the Equation of Motion of a SDOF system.

2.2 Undamped Free Vibrations

The motion of a SDOF system free from external action or forces is governed by the initial conditions. If damping is disregarded the equation of motion (2.5) is of the form:

$$m \cdot \ddot{q}(t) + k \cdot q(t) = 0 \tag{2.6}$$

This is a homogeneous second order linear differential equation with constant coefficients.

Considering solutions of the form

$$q(t) = A \cdot \cos(\omega \cdot t) \tag{2.7}$$

or

$$q(t) = B \cdot sin(\omega \cdot t) \tag{2.8}$$

where A and B are constants, one may easily verify by direct substitution, that these are solutions to the differential equation (2.6). For instance, the substitution of equation (2.7) into (2.6) leads to:

$$\left(- m \cdot \omega^2 + k\right) \cdot A \cdot \cos(\omega \cdot t) = 0 \tag{2.9}$$

In order to satisfy this condition at any time *t*, the term in the first parenthesis must be equal to zero, giving:

$$\omega = \sqrt{\frac{k}{m}} \tag{2.10}$$

Since the differential equation (2.6) is linear and homogeneous, the superposition of the two solutions above is also a solution. Therefore one may write the general solution as:

$$q(t) = A \cdot sin(\omega \cdot t) + B \cdot cos(\omega \cdot t) \tag{2.11}$$

[3] Damping forces are always present in any physical system undergoing motion. These forces are part of a mechanism transforming the mechanical energy of the system to other forms of energy such as heat. The mechanism is quite complex and still not completely understood. Therefore the damping influence is usually quantified on the basis of experience.

The constants of integration *A* and *B* may be expressed in terms of the initial conditions, i.e. the displacement, *q(0)*, and the velocity, $\dot{q}(0)$, at time *t=0*. Thus the solution becomes:

$$q(t) = \frac{\dot{q}(0)}{\omega} \cdot sin(\omega \cdot t) + q(0) \cdot cos(\omega \cdot t) \tag{2.12}$$

This last equation is the equation for the motion of an undamped SDOF system under free-vibration conditions. This is a simple harmonic motion, in which the quantity ω is the circular frequency. Dividing ω by the factor $2 \cdot \pi$, one obtains the *natural frequency of the system*, *f*, expressed in Hz (cycles per second). As shown by expression (2.10), this parameter only depends on the system properties *k* and *m*.

Expression (2.12) may be used qualitatively to understand how the response is influenced by the stiffness and inertia properties of the system as well as the initial conditions:

- A very stiff (or very "light") SDOF system has a large value of *k* (or low value for *m*), and so the response frequency is high and the displacements are mainly given by $q(t) \doteq q(0) \cdot \cos(\omega \cdot t)$. Consequently the maximum displacement will be of the same order as the initial displacement, *q(0);*
- A very flexible (or very "heavy") SDOF system has a large value for m (or low value of k). The response frequency is low and the maximum displacement is mainly governed by $q(t) \doteq \frac{\dot{q}(0)}{\omega} \cdot sin(\omega \cdot t)$. This implies that the maximum displacements may be larger than the initial displacement, *q(0)*.

2.3 Damped free vibrations

We now discuss a SDOF system vibrating freely but we include the effect of the damping forces. The equation of motion (2.5) then has the form:

$$m \cdot \ddot{q}(t) + c \cdot \dot{q}(t) + k \cdot q(t) = 0 \tag{2.13}$$

This differential equation is of the same form as before for the undamped case, but the solution now is:

$$q(t) = C \cdot e^{s \cdot t} \tag{2.14}$$

where *C* is a constant. This is proved substituting (2.14) into (2.13) which leads to

$$\left(m \cdot s^2 + c \cdot s + k\right) \cdot C \cdot e^{s \cdot t} = 0 \tag{2.15}$$

Requiring the parenthesis to be zero we get:

$$m \cdot s^2 + c \cdot s + k = 0 \tag{2.16}$$

The roots of this quadratic equation are:

$$\left.\begin{matrix} S_1 \\ S_2 \end{matrix}\right\} = -\frac{c}{2 \cdot m} \pm \sqrt{\left(\frac{c}{2 \cdot m}\right)^2 - \omega^2} \tag{2.17}$$

As in the previous paragraph, the general solution is given by superposition of the two possible solutions:

$$q(t) = C_1 \cdot e^{s_1 \cdot t} + C_2 \cdot e^{s_2 \cdot t} \tag{2.18}$$

Depending on the value of *c*, one gets three types of motion, according to the quantity under the square-root sign being positive, negative or zero.

The value making the square-root quantity zero is called the critical damping value, $c_c = 2 \cdot m \cdot \omega$, and it may be shown that this value represents the largest value of damping that leads to oscillatory motion in free response. Structural systems under normal conditions do not have values of damping above this critical value. So, in the following, only the situation for *underdamped systems* will be discussed, i.e. systems with damping below the critical value.

Under these conditions, equation (2.18) may be written in a more convenient form, introducing the parameters:

- ξ, which is the damping ratio to the critical damping value i.e. $\xi = \frac{c}{2 \cdot m \cdot \omega}$
- ω_d, the damped vibration frequency, i.e. $\omega_d = \omega \cdot \sqrt{1 - \xi^2}$

$$q(t) = e^{-\xi \cdot \omega \cdot t} \left[A \cdot (\omega_d \cdot t) + B \cdot sin(\omega_d \cdot t) \right] \tag{2.19}$$

Finally, when the initial condition of displacement, q_0, and velocity, $\dot{q}_0$, are introduced, the constant of integration *A* and *B* can be evaluated and substituted into equation (2.19), giving:

$$q(t) = e^{-\xi \cdot \omega \cdot t} \left[q_0 \cdot cos(\omega_d \cdot t) + \frac{\dot{q}_0 + q_0 \cdot \xi \cdot \omega}{\omega_d} \cdot sin(\omega_d \cdot t) \right] \tag{2.20}$$

The term in parenthesis represents simple harmonic motion, as it is of the same form as equation (2.12). It is of interest to note that the frequency for this harmonic motion is now given by ω_d with the expression as above. For common structural systems (ξ <20%) this value differs very little from the undamped frequency as shown by equation (2.10), so it may be inferred that, for normal conditions, damping will not have any significant influence on the frequency of motion.

The effect of damping is more evident when considering the successive peak responses (see figure 2). It may be shown that the ratio between two successive peaks, q_n and q_{n+1}, is given approximately by:

$$\frac{q_{n+1}}{q_n} \cong e^{-2 \cdot \pi \cdot \xi} \tag{2.21}$$

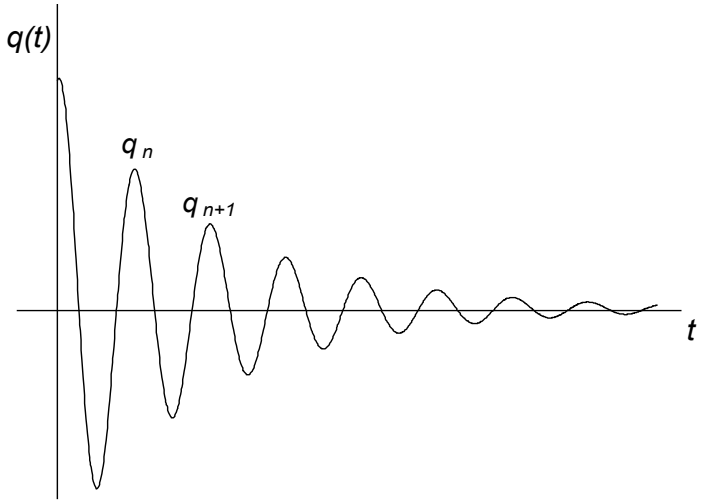

Figure 2 – Plot of a free-vibration response equation of motion for underdamped SDOF systems

We may now formulate the equation of motion for SDOF systems by introducing the damping ratio, ξ, and the natural vibration frequency, ω:

$$\ddot{q}(t) + 2 \cdot \xi \cdot \omega \cdot \dot{q}(t) + \omega^2 \cdot q(t) = \frac{p(t)}{m} \tag{2.22}$$

2.4 Resonant Response[4]

To explain this important phenomenon, taking place when a structure is submitted to dynamical loading, response to harmonic loading will be considered.

The simplest load of this type is of the form:

$$p(t) = p_0 \cdot sin(\overline{\omega} \cdot t) \tag{2.23}$$

where p_0 is the maximum value and $\overline{\omega}$ its frequency

The equation of motion (2.5) may now be written as follows:

$$m \cdot \ddot{q}(t) + c \cdot \dot{q}(t) + k \cdot q(t) = p_0 \cdot sin(\overline{\omega} \cdot t) \tag{2.24}$$

[4] The study of SDOF systems cannot be completed without discussing the equations of motion for harmonic and periodic loading. However these subjects are not directly related to the standard methods for seismic design to be presented in this document. The reader is referred to, for example, chapters 4 and 5 of reference 1 or chapter 3 of reference 2.

One has now a non-homogenous differential equation which solution is of the form:

$$q(t) = e^{-\xi \cdot \omega \cdot t} \cdot \left[A \cdot sin(\omega_d \cdot t) + B \cdot cos(\omega_d \cdot t)\right] + \\ + \frac{p_0}{k} \cdot \frac{\left[\left(1-\beta^2\right) \cdot sin(\overline{\omega} \cdot t) - 2 \cdot \xi \cdot \beta \cdot cos(\overline{\omega} \cdot t)\right]}{\left(1-\beta^2\right)^2 + (2 \cdot \xi \cdot \beta)^2} \qquad (2.25)$$

Here:

A and *B* have the same meaning as before i.e. they depend on the initial conditions.

The parameter β is defined as the ratio $\beta = \frac{\overline{\omega}}{\omega}$.

The first term in (2,25) is called *the transient response* and because of its dependence on the factor $e^{-\xi \cdot \omega \cdot t}$,it damps out quickly. Therefore its evaluation is of little interest for the present discussion.

The second term is called *the steady-state response* and it may be written in a more convenient form:

$$q(t) = \rho \cdot sin(\overline{\omega} \cdot t - \theta) \qquad (2.26)$$

The term ρ is the amplitude, i.e. the maximum value of the displacement. It may be shown that this value is given in terms of the static displacement $\frac{p_0}{k}$ multiplied by the factor, *D*, which is called *dynamical magnification* factor:

$$\rho = \frac{p_0}{k} \cdot D \qquad (2.27)$$

with *D* expressed as:

$$D = \frac{1}{\sqrt{\left(1-\beta^2\right)^2 + (2 \cdot \xi \cdot \beta)^2}} \qquad (2.28)$$

The value θ is called the phase angle and describes how the response lags behind the applied load:

$$\theta = tan^{-1}\left(\frac{2 \cdot \xi \cdot \beta}{1-\beta^2}\right) \qquad (2.29)$$

Several plots of the dynamical magnification factor with respect to β are shown in figure 3 for values of damping, ξ , usually found in common structures.

As it may be seen the peak values of *D* are reached when β is very close to 1 (in fact, when $\beta = \sqrt{1-2 \cdot \xi^2}$). This means that when the load frequency approaches the natural vibration frequency of the SDOF system, the response will increase more and more. This phenomenon is called *resonance*.

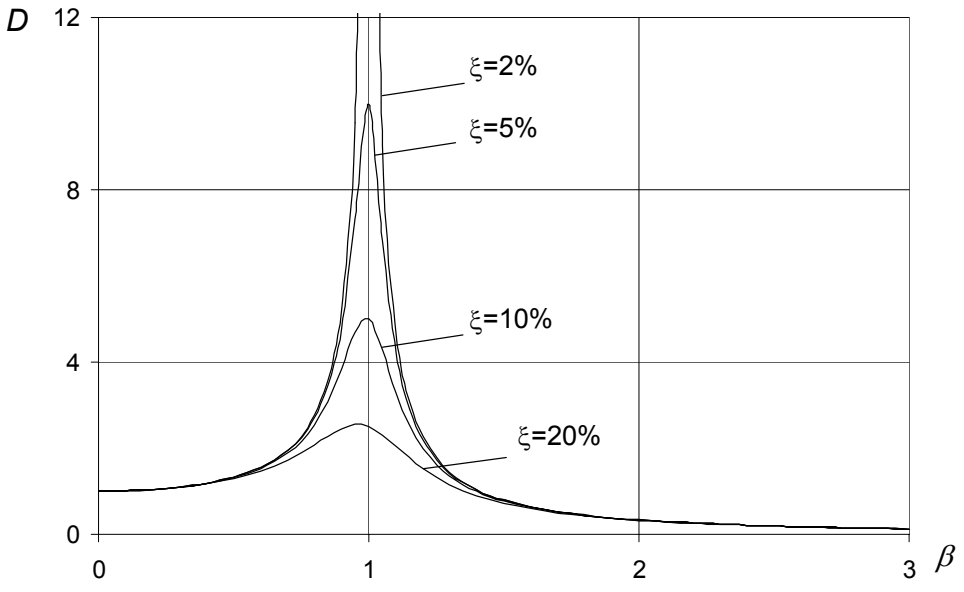

Figure 3 – The dynamical magnification factor ***D*** as a function of β

Substituting the value of β for which *D* is maximum, one has the following expression for the maximum response, q_{max}:

$$q_{max} = \frac{1}{2 \cdot \xi \cdot \sqrt{1-\xi^2}} \cdot \frac{p_0}{k} \tag{2.30}$$

The effect of damping on the resonant response is seen clearly: The lower is the damping value, ξ, the bigger the response. Theoretically for undamped conditions the value is infinite.

The physical explanation for resonance is of course that both load frequency and natural vibration frequency of the system are so close that most part of the time the response and the load signals are in the same phase. This means that when the system is moving in a certain direction the load is in the same direction. This will lead to a consecutive amplification of the response in each cycle until the limit given by expression (2.30) is reached. For undamped conditions the response will grow indefinitely.

It should be also noticed that for values of β near *0*, i.e. when the natural vibration frequency of the system is much higher than the load frequency, *D* approaches unity. This means that the response will be closer to the static response. In fact, for highly stiff systems the quantity $k \cdot q(t)$ is expected to play an important role in the final response.

2.5 Base Motion for SDOF Systems

Figure 4 shows a sketch of a SDOF system when submitted to base motion.

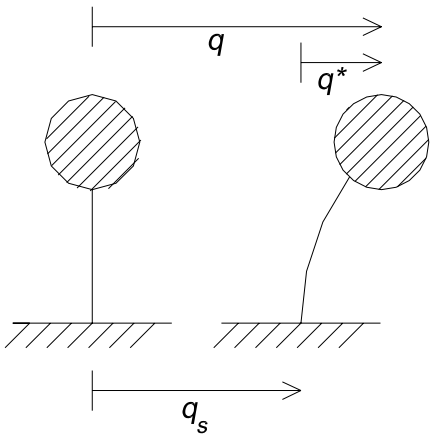

Figure 4 – SDOF system submitted to base motion

When a SDOF system is submitted to base motion, one may write the absolute displacement, q, in terms of the sum of the relative displacement, q^*, and the support displacement, q_s (figure 4).

$$q = q^* + q_s \tag{2.31}$$

The formulation of the equation of motion leads to the same form as (2.2). However it should be noted that no load is acting on the system. The only action able to induce deformation on the system is the support displacement, q_s. Therefore, as in (2.2), one may write the dynamical equilibrium condition:

$$f_i + f_c + f_k = 0 \tag{2.32}$$

Here:

- Inertia forces, f_k, are in terms of absolute coordinates, $\ddot{q}$.
- Elastic forces, f_k, and damping forces, f_c, are in terms of relative coordinates, q^* and $\dot{q}^*$, respectively.

$$m \cdot \ddot{q}(t) + c \cdot \dot{q}^*(t) + k \cdot q^*(t) = 0 \tag{2.33}$$

By means of (2.31) it's possible to write the previous equation in terms of relative coordinates. This is more convenient for the purpose of achieving the effects on the system due to base motion:

$$m \cdot \ddot{q}^*(t) + c \cdot \dot{q}^*(t) + k \cdot q^*(t) = -m \cdot \ddot{q}_s(t) \tag{2.34}$$

Equation (2.34) is of the same form as (2.5). Therefore the response analysis of a SDOF system submitted to ground motion, in terms of relative coordinates, may be treated assuming a load applied on the system equal to $p(t) = -m \cdot \ddot{q}_s(t)$.

Equation (2.34) may also be formulated in the same way as (2.22):

$$\ddot{q}^*(t) + 2 \cdot \xi \cdot \omega \cdot \dot{q}^*(t) + \omega^2 \cdot q^*(t) = -\ddot{q}_s(t) \tag{2.35}$$

Again we have a non-homogeneous differential equation and so it is necessary to find a particular solution, which depends on the form of $\ddot{q}_s(t)$. In chapter 4, the solution for base acceleration of general form will be discussed.

2.6 Formulation of the Equation of Motion for MDOF systems

From the discussion in the previous paragraphs, a degree of freedom is defined as an independent coordinate, necessary to specify the configuration or position of a system at any time, *q(t)*.

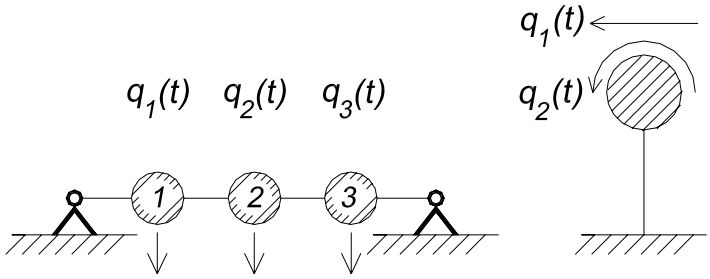

Figure 5 – Examples of MDOF systems

A structural system composed by more than one degree of freedom is called a Multi--Degree of Freedom system (MDOF). Figure 5 shows two examples of MDOF systems.

The establishment of the equations of motion for several degrees of freedom proceeds analogously as for the SDOF systems, which leads to a dynamical equilibrium condition of the same form as (2.2) for each degree of freedom. The result is a system of *N* differential equations, in which *N* is the number of degrees of freedom.

$$\begin{aligned} f_{i,1} + f_{c,1} + f_{k,1} &= p_1(t) \\ f_{i,2} + f_{c,2} + f_{k,2} &= p_2(t) \\ &\cdots\cdots\cdots\cdots \\ f_{i,N} + f_{c,N} + f_{k,N} &= p_N(t) \end{aligned} \tag{2.36}$$

Each of the resisting forces, $f_{i,i}$, $f_{c,i}$ or $f_{k,i}$ developed for a certain degree of freedom, *i*, is due to the motion of one degree of freedom. For example the elastic force produced for the degree of freedom *1*, $f_{k,1}$, is the sum of the different elastic forces acting at point *1*, each one due to the displacement of each of any of the other degrees of freedom.

Most conveniently the resisting forces may be expressed by means of a set of influence coefficients. Considering again the example above one has:

$$f_{k,1} = \sum_{i=1}^{N} k_{1i} \cdot q_i(t) \tag{2.37}$$

in which k_{1i} is called the stiffness influence coefficient. It may be defined as the force at degree of freedom 1 due to a unit *displacement* corresponding to degree of freedom *i*.

In figure 6 is illustrated the analysis of the stiffness coefficients in a two-storey frame with masses M_1 and M_2, bending stiffness of the columns EI and lengths of the columns L.

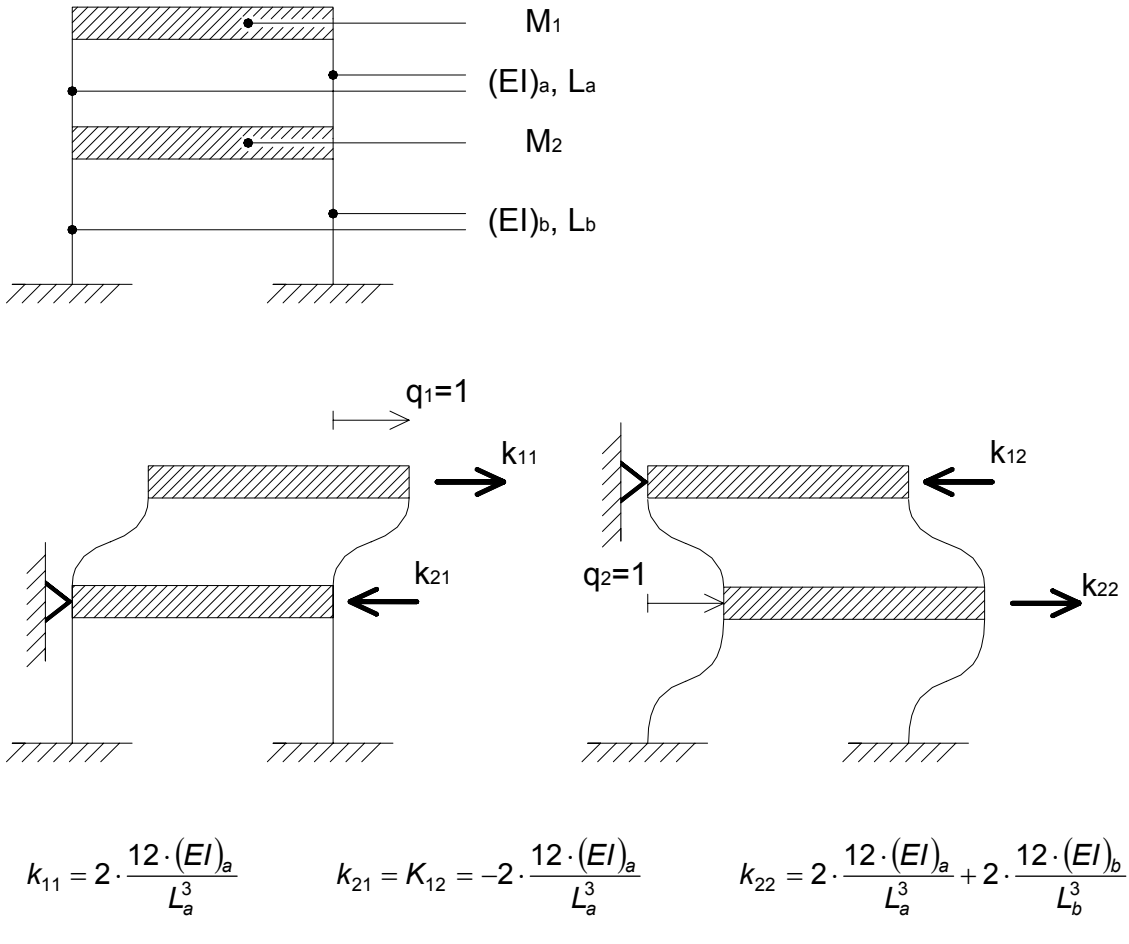

$$k_{11} = 2 \cdot \frac{12 \cdot (EI)_a}{L_a^3} \qquad k_{21} = K_{12} = -2 \cdot \frac{12 \cdot (EI)_a}{L_a^3} \qquad k_{22} = 2 \cdot \frac{12 \cdot (EI)_a}{L_a^3} + 2 \cdot \frac{12 \cdot (EI)_b}{L_b^3}$$

Figure 6 – Analysis of frame stiffness coefficients

Analogously one may define the damping forces produced for degree of freedom 1:

$$f_{c,1} = \sum_{i=1}^{N} c_{1i} \cdot \dot{q}_i(t) \tag{2.38}$$

in which c_{1i} are called the damping influence coefficients. They may be defined as the force at degree of freedom 1 due to unit *velocity* of the degree of freedom *i*.

Finally the inertia forces produced for degree of freedom 1:

$$f_{i,1} = \sum_{i=1}^{N} m_{1i} \cdot \ddot{q}_i(t) \tag{2.39}$$

in which m_{1i} are called the mass influence coefficients and may be defined as the force at degree of freedom 1 due to unit *acceleration* corresponding to degree of freedom *i*.

It is important to notice that the principle of superposition may be applied only if linear behaviour is assumed.

The set of equations in (2.36) may be written in matrix form:

$$[M] \cdot \{\ddot{q}(t)\} + [C] \cdot \{\dot{q}(t)\} + [K] \cdot \{q(t)\} = \{p(t)\} \tag{2.40}$$

This equation is equivalent to (2.5) for a given MDOF system as it expresses the *N* equations of motion defining its response[5]. In the following paragraphs until 2.11 the procedures leading to the solution of this system will be discussed.

2.7 Frequency and Vibration Mode Shape Analysis

The problem of determining the vibration frequencies in MDOF systems is solved as for SDOF systems, i.e. assuming undamped conditions and no loads applied. For this situation equation (2.40) is written as follows:

$$[M] \cdot \{\ddot{q}(t)\} + [K] \cdot \{q(t)\} = 0 \tag{2.41}$$

By analogy with the behaviour of SDOF systems, it is assumed that the free-vibration motion response is simple harmonic, i.e. of the form (2.12):

$$\{q(t)\} = \{\overline{q}\} \cdot sin(\omega \cdot t + \theta) \tag{2.42}$$

Here

$\{\overline{q}\}$ represents the vibration shape of system, (constant in time)
ω is the vibration frequency and
θ the phase angle.

Introducing the equation of motion into (2.41) and observing that $\{\ddot{q}(t)\} = -\omega^2 \{\overline{q}\} \cdot \sin(\omega \cdot t + \theta)$ one has (after omitting the sine term):

$$\left[K - \omega^2 \cdot M\right] \cdot \{\overline{q}\} = 0 \tag{2.43}$$

[5] For further study of the formulation of the equations of motion for MDOF systems, the reader is referred to chapter 11 in reference 1 regarding the evaluation of the matrices [M], [C] and [K] .

The only non-trivial solution of this equation is the one making the determinant of the matrix $\left[K - \omega^2 \cdot M\right]$ equal to *0*, (2.44). Thus the problem of determining the frequencies in a MDOF system results in an eigenvalue problem of the non-standard form. The eigenvalues are the squares of the frequencies and the eigenvectors are the vibration modes associated with the frequencies.

$$\left\|K - \omega^2 \cdot M\right\| = 0 \tag{2.44}$$

Equation (2.44) is called the *frequency equation* for MDOF systems. Expanding the determinant gives a polynomial expression of the *N*th degree. Therefore one has a set of *N* solutions $\left(\omega_1^2, \omega_2^2, ..., \omega_N^2\right)$, each one representing a possible vibration mode. Each shape vector, $\{\overline{q}\}$, is determined substituting the corresponding frequency, ω_i, into equation (2.43).

The lowest frequency (also called *the natural frequency*) corresponds to the first vibration mode, the next higher corresponds to the second vibration mode, etc.

It is of interest to notice that, as for SDOF systems, the frequencies and the corresponding vibration mode shape depend only on the mass, $[M]$, and the stiffness, $[K]$, of the system.

It should also be noticed that the system resulting from substituting a given frequency, ω_i, into equation (2.43) is homogeneous, with linear dependent equations and therefore indeterminate. This means that it's impossible to determine the amplitudes of each degree of freedom in the corresponding vibration shape by simply resorting to equation (2.43). Only ratios between these amplitudes may be established.

It is obvious that there are infinitely many ways of computing the relations between the values of each vibration mode shape. It is usual to do it so to obtain an easy interpretation and comparison of the several vibration modes.

One of these ways is to normalize the vectors so that the largest value corresponds to unity. Another way is to assign the same value for a given degree of freedom in each vibration mode vector.

Either way it is convenient to express the vibration mode shapes in the normalized form, i.e., in dimensionless terms by dividing all the components by one reference component. The resulting vector is called the *n*th mode shape ϕ_n. The matrix, $[\Phi]$, assembling each of the mode shapes in a column is called *the mode shape matrix* and may be written as follows:

$$[\Phi] = \begin{bmatrix} \phi_{11} & \phi_{12} & \cdots & \phi_{1N} \\ \phi_{21} & \phi_{22} & \cdots & \phi_{2N} \\ \cdots & \cdots & \cdots & \cdots \\ \phi_{N1} & \phi_{N2} & \cdots & \phi_{NN} \end{bmatrix} \tag{2.45}$$

2.8 Orthogonality Conditions

The free vibration mode shape vectors, ϕ_n, have certain special properties called orthogonality conditions, which are very useful in structural dynamical analysis.

Orthogonality with respect to the mass matrix

The dynamical equilibrium equation in the form (2.43) may be written for the modes *n* and *m* as follows.

$$[K]\cdot\phi_n = \omega_n^2\cdot[M]\cdot\phi_n \tag{2.46}$$

$$[K]\cdot\phi_m = \omega_m^2\cdot[M]\cdot\phi_m \tag{2.47}$$

Multiplying equation (2.46) by ϕ_m^T one has:

$$\phi_m^T\cdot[K]\cdot\phi_n = \omega_n^2\cdot\phi_m^T\cdot[M]\cdot\phi_n \tag{2.48}$$

Transposing equation (2.47) and noticing that $[M]$ and $[K]$ are symmetrical, i.e.: $[M]=[M]^T$ and $[K]=[K]^T$, one has:

$$\phi_m^T\cdot[K]=\omega_m^2\cdot\phi_m^T\cdot[M] \tag{2.49}$$

If equation (2.49) is multiplied on the right-hand side of each member by ϕ_n, the following expression is achieved:

$$\phi_m^T\cdot[K]\cdot\phi_n = \omega_m^2\cdot\phi_m^T\cdot[M]\cdot\phi_n \tag{2.50}$$

Subtracting equation (2.50) from equation (2.48) results in:

$$\left(\omega_n^2-\omega_m^2\right)\cdot\phi_m^T\cdot[M]\cdot\phi_n = 0 \tag{2.51}$$

It is evident from the discussion in paragraph 2.7 that if $m \neq n$, the corresponding frequencies will be different, making the following equation (2.52) valid:

$$\phi_m^T\cdot[M]\cdot\phi_n = 0 \tag{2.52}$$

This condition shows that the vibration mode shapes are orthogonal with respect to the mass matrix.

Orthogonality with respect to the stiffness matrix

Dividing equations (2.48) and (2.50) by ω_n^2 and ω_m^2, respectively, one has:

$$\frac{1}{\omega_n^2}\cdot\phi_m^T\cdot[K]\cdot\phi_n = \phi_m^T\cdot[M]\cdot\phi_n \tag{2.53}$$

$$\frac{1}{\omega_m^2}\cdot\phi_m^T\cdot[K]\cdot\phi_n = \phi_m^T\cdot[M]\cdot\phi_n \tag{2.54}$$

Subtracting equation (2.54) from (2.53) gives the following condition:

$$\left(\frac{1}{\omega_n^2}-\frac{1}{\omega_m^2}\right)\cdot\phi_m^T\cdot[K]\cdot\phi_n=0 \tag{2.55}$$

Thus for different vibration mode shapes the following orthogonality condition with respect to the stiffness matrix is valid:

$$\phi_m^T\cdot[K]\cdot\phi_n=0 \tag{2.56}$$

The results (2.52) and (2.56) lead to:

$$[\Phi]^T\cdot[M]\cdot[\Phi]=[M]_G \tag{2.57}$$

$$[\Phi]^T\cdot[K]\cdot[\Phi]=[K]_G \tag{2.58}$$

in which the matrices $[M]_G$ and $[K]_G$ are of diagonal form.

2.9 Modal Coordinates

For dynamical analysis of linear systems with any kind of property (damped or undamped; with or without loading) it is assumed that the displacements are represented in terms of the free vibration mode shapes, ϕ_n. These shapes constitute *N* independent displacement patterns, the amplitudes of which may serve as generalized coordinates to express any form of displacement. This is the same to say that any displacement vector, $\{q\}$, may be written by superimposing suitable amplitudes, *Y*, of the *N* modes of vibration.

$$\begin{aligned}\{q\}&=\phi_1\cdot Y_1+\phi_2\cdot Y_2+\ldots+\phi_N\cdot Y_N\Leftrightarrow\\ \Leftrightarrow\{q\}&=\sum_{n=1}^{N}\phi_n\cdot Y_n\end{aligned} \tag{2.59}$$

It is evident that the mode-shape matrix serves to transform from the generalised coordinates, *Y*, to the geometric coordinates, *q*. These generalized mode-amplitude coordinates are called *modal coordinates*.

$$\{q\}=[\Phi]\cdot\{Y\} \tag{2.60}$$

The problem lies now in determining the modal coordinates vector, $\{Y\}$, so that it may be used in equation (2.60) in order to determinate the response of the system in geometrical coordinates. The procedure of determining the displacement vector, $\{q\}$ using (2.60) is called *mode superposition method*.

It should be noted that the mode-shape matrix, $[\Phi]$, is composed by *N* independent modal vectors and therefore it is non-singular and may be inverted. This means that

it may always be solved directly for the modal coordinates amplitude, *Y,* associated with any given displacement vector, $\{q\}$.

$$\{Y\} = [\Phi]^{-1} \cdot \{q\} \tag{2.61}$$

2.10 Equation of Motion in Modal Coordinates

The equation of motion (2.40) represents a set of *N* simultaneous differential equations coupled by the off-diagonal terms in the mass and stiffness matrices. It will now be shown that, with an appropriate normalizing procedure for the vectors ϕ_n and regarding the orthogonality conditions observed previously, it is possible to transform the equation of motion into a set of *N* independent modal coordinate equations. Solving each of these equations and applying the mode superposition method leads to the establishment of the dynamical response of the system.

The normalising procedure is called *normalization with respect to the mass matrix,* $[M]$, and may consist in writing the vibration mode shape vector, ϕ_n, so that the following condition will be valid:

$$\phi_n^T \cdot [M] \cdot \phi_n = 1 \tag{2.62}$$

In order to determine, ϕ_n, the reference component by which the *n*th vibration mode shape, $\{\overline{q}\}_n$, should be divided is:

$$\sqrt{\{\overline{q}\}_n^T \cdot [M] \cdot \{\overline{q}\}_n} \tag{2.63}$$

Finally the normalized vibration mode shape vector ϕ_n:

$$\phi_n = \frac{\{\overline{q}\}_n}{\sqrt{\{\overline{q}\}_n^T \cdot [M] \cdot \{\overline{q}\}_n}} \tag{2.64}$$

As a consequence of this normalization, using (2.62), one has:

$$[\Phi]^T \cdot [M] \cdot [\Phi] = [I] \tag{2.65}$$

with $[I]$ as the *N* x *N* identity matrix.

Another important result deriving from this type of normalization may also be shown:

1) Multiplying both members of equation (2.46) by ϕ_n^T, one obtains:

$$\phi_n^T \cdot [K] \cdot \phi_n = \omega_n^2 \cdot \phi_n^T \cdot [M] \cdot \phi_n \tag{2.66}$$

2) Using the result expressed in (2.65) and remembering (2.58),

$$\phi_n^T \cdot [K] \cdot \phi_n = \omega_n^2 \quad \Rightarrow \quad K_{G,n} = \omega_n^2 \tag{2.67}$$

Therefore, the diagonal element at line *n* of the stiffness matrix, $[K]_G$, equals the square of the *n*th vibration mode frequency.

Regarding damping, it will be assumed that, as for the mass and stiffness matrices, the damping matrix is written in a way that the orthogonality conditions are satisfied:

$$[\Phi]^T \cdot [C] \cdot [\Phi] = [C]_G \tag{2.68}$$

It may be shown that, if the mode shape matrix, $[\Phi]$, is normalized according to (2.64), then the matrix $[C]_G$ is a diagonal matrix with each diagonal element $c_{G,nn}$ as:

$$c_{G,nn} = \phi_n^T \cdot [C] \cdot \phi_n = 2 \cdot \omega_n \cdot \xi_n \tag{2.69}$$

where ξ_n represents the *n*th mode damping ratio. This parameter may be interpreted as an energy loss mechanism associated with the corresponding vibration mode[6].

In the following the steps that allow writing equation (2.40) in terms of modal coordinates and therefore as a set of independent equations are described.

1) Equation of motion in terms of the geometrical coordinates.

$$[M] \cdot \{\ddot{q}(t)\} + [C] \cdot \{\dot{q}(t)\} + [K] \cdot \{q(t)\} = \{p(t)\} \tag{2.40}$$

2) Multiplication of both members by $[\Phi]^T$ and introduction of the neutral element $[\Phi] \cdot [\Phi]^{-1} = [I]$ in the first member.

$$\begin{aligned} [\Phi]^T \cdot [M] \cdot [\Phi] \cdot [\Phi]^{-1} \cdot \{\ddot{q}(t)\} + [\Phi]^T \cdot [C] \cdot [\Phi] \cdot [\Phi]^{-1} \cdot \{\dot{q}(t)\} + \\ + [\Phi]^T \cdot [K] \cdot [\Phi] \cdot [\Phi]^{-1} \cdot \{q(t)\} = [\Phi]^T \cdot \{p(t)\} \end{aligned} \tag{2.70}$$

3) Simplification considering the results (2.65), (2.58) and (2.68).

$$[\Phi]^{-1} \cdot \{\ddot{q}(t)\} + [C]_G \cdot [\Phi]^{-1} \cdot \{\dot{q}(t)\} + [K]_G \cdot [\Phi]^{-1} \cdot \{q(t)\} = [\Phi]^T \cdot \{p(t)\} \tag{2.71}$$

It is evident now that one may write the previous equation for the modal coordinate, Y_n, considering the transformation expressed in (2.61) and simplifying by means of (2.67) and (2.69), in the following form.

$$\ddot{Y}_n + 2 \cdot \omega_n \cdot \xi_n \cdot \dot{Y}_n + \omega_n^2 \cdot Y_n = \phi_n^T \cdot \{p(t)\} \tag{2.72}$$

Two comments should be made about this equation:

i. The mode shape matrix, $[\Phi]$, does not change with time which implies:

$$\{\dot{Y}\} = [\Phi]^{-1} \cdot \{\dot{q}(t)\} \tag{2.73}$$

[6] The conditions regarding damping orthogonality are discussed in detail in chapter 13-3 of reference 1 and section 12.3 of reference 2.

$$\left\{\ddot{Y}\right\} = \left[\Phi\right]^{-1} \cdot \left\{\ddot{q}(t)\right\} \tag{2.74}$$

ii. Equation (2.72) is written in terms of modal coordinates, in which the normalizing procedure has been done with respect to the mass matrix. Therefore the following equation may be inferred from (2.72) using (2.57) and (2.65):

$$\ddot{Y}_n + 2 \cdot \omega_n \cdot \xi_n \cdot \dot{Y}_n + \omega_n^2 \cdot Y_n = \frac{\phi_n^T \cdot \left\{p(t)\right\}}{M_{G,n}} \tag{2.75}$$

The similarity between the previous expression and equation (2.22), describing the equation of motion for SDOF systems, is evident. This similarity is the basic principle for carrying out a dynamical analysis using the mode superposition method assuming that the system behaves linearly. In fact it is assumed that the motion response for the mode *n* (modal coordinate Y_n) is the same as the motion response computed for a SDOF system with the properties *m*, ω and ξ having the same values as the corresponding ones written in modal coordinates $M_{G,n}$, ω_n and ξ_n. As already discussed in the chapters referring to SDOF systems it is possible to solve equations (2.72) or (2.75) for each of the *N* modes and therefore achieve the modal coordinates vector $\left\{Y\right\}$. As mentioned before, once the vector $\left\{Y\right\}$ is determined, application of the transformation (2.60) leads to the global response of the system in terms of single degree of freedom equations in geometric coordinates.

However, for common structural systems subjected to extreme dynamical loading, as in a strong earthquake, it may be rather unrealistic to assume linear behaviour. For instance, in reinforced concrete structures submitted to dynamic loading, the stiffness distribution successively changes, not only due to the fact that certain elements are near yielding but also due to cracking. These are effects very difficult to take into account with the mode superposition method, since this method assumes that the structural properties remain constant in time. Therefore no information beyond the elastic limit is provided such as the inelastic energy dissipation. It is known that the formation of plastic hinges in a structure designed in a redundant way leads to the dissipation of energy transmitted by dynamic loading. This has a similar effect as damping and has a significant contribution to the structural response after yielding.

2.11 Base Motion for MDOF Systems

The establishment of the equations of motion for several degrees of freedom MDOF systems follows the reasoning described above. Again, relative coordinates, *q**, presented in (2.31), are used due to the convenience regarding the effects of base motion on the system.

Because no dynamic load is applied on any degree of freedom, the set of equations of motion, in the form of (2.36), will be written as follows:

$$\begin{aligned} &f_{i,1} + f_{c,1} + f_{k,1} = 0 \\ &f_{i,2} + f_{c,2} + f_{k,2} = 0 \\ &\ldots\ldots\ldots\ldots\ldots\ldots \\ &f_{i,N} + f_{c,N} + f_{k,N} = 0 \end{aligned} \tag{2.76}$$

As in SDOF systems, only the inertia forces, $f_{i,i}$, are in terms of absolute coordinates. Reducing (2.76) to relative coordinates and expressing the equation in matrix form leads to:

$$[M]\cdot\{\ddot{q}^*(t)\} + [C]\cdot\{\dot{q}^*(t)\} + [K]\cdot\{q^*(t)\} = -[M]\cdot\{\ddot{q}_s(t)\}^7 \tag{2.77}$$

The vector $\{\ddot{q}_s(t)\}$ is the support acceleration vector and depends on the particular support conditions. However, it is reasonable to neglect this fact due to simplification regarding the common structural dimensions.

It should also be noted that the support acceleration vector has three components $\{\ddot{q}_{sX}(t)\}$, $\{\ddot{q}_{sY}(t)\}$ and $\{\ddot{q}_{sZ}(t)\}$, corresponding to direction *X*, *Y*, and *Z*. It will be assumed here that the first two directions are in the surface plane and *Z* corresponds to vertical direction.

Referring to the explanation, given in paragraph 2.6 about the influence coefficients, $m_{i,i}$, $c_{i,i}$ and $k_{i,i}$, composing the matrices $[M]$, $[C]$ and $[K]$, it is evident that if a degree of freedom, *i*, is under direction *J*, only the motion of the degrees of freedom under *J* direction will affect the motion of the actual degree of freedom *i*. Therefore it is practical to introduce into equation of motion (2.77) a set of vectors $\{1_X\}$, $\{1_Y\}$ and $\{1_Z\}$. These are written so that *n*th line corresponds to the *n*th degree of freedom and the corresponding value will be unity, if the degree of freedom is in the same direction as that of the vector, otherwise it is zero.

Introducing the above vectors the equation of motion for MDOF systems submitted to base motion will have the following form:

$$\begin{aligned} [M]\cdot\{\ddot{q}(t)\} + [C]\cdot\{\dot{q}(t)\} + [K]\cdot\{q(t)\} = \\ = -[M]\cdot\left(\{1_X\}\cdot\ddot{q}_{sX}(t) + \{1_Y\}\cdot\ddot{q}_{sY}(t) + \{1_Z\}\cdot\ddot{q}_{sZ}(t)\right) \end{aligned} \tag{2.78}$$

It is obvious that this equation is of the same form as (2.40). The procedures described in the previous paragraph, regarding the equation of motion in modal coordinates, may then be applied. Considering again the *n*th modal coordinate, one has:

---

[7] In the present document whenever support motion is discussed for MDOF systems, the relative coordinates are used. Therefore the symbol * will be omitted in the following expressions.

$$\begin{aligned}\ddot{Y}_n + 2\cdot\omega_n\cdot\xi_n\cdot\dot{Y}_n + \omega_n^2\cdot Y_n = \\ = -\phi_n^T\cdot[M]\cdot\{1_X\}\cdot\ddot{q}_{sX}(t) - \phi_n^T\cdot[M]\cdot\{1_Y\}\cdot\ddot{q}_{sY}(t) - \phi_n^T\cdot[M]\cdot\{1_Z\}\cdot\ddot{q}_{sZ}(t)\end{aligned} \tag{2.79}$$

The term $\phi_n^T\cdot[M]\cdot\{1_j\}$, affecting each acceleration value $\ddot{q}_{sJ}$, is denominated *the modal participation factor of the nth mode for direction J, P_{nJ}*. As it may be inferred it only depends on the vibration mode shape, the mass distribution and the direction of each degree of freedom. By superposition analysis, regarding the linear behaviour of the system, is possible to solve the equation separately for each direction, which will lead, for mode *n* and direction *J*, to the following differential equation.

$$\ddot{Y}_n + 2\cdot\omega_n\cdot\xi_n\cdot\dot{Y}_n + \omega_n^2\cdot Y_n = -P_{nJ}\cdot\ddot{q}_{sJ}(t) \tag{2.80}$$

It was mentioned before that the support motion from an earthquake is of the form of an excitation. Therefore the minus sign in (2.80) is of minor interest. Generally the sign of the response does not have any important significance in an earthquake analysis. From now on it will be omitted due to simplification.

Equation (2.80) is of the same form as (2.72), which means that it may be solved analogously as for a SDOF system. Moreover, as the modal participation factor is a dimensionless parameter and the behaviour of the system is linear, it is possible to solve the equation of motion in the form (2.80) without using P_{nj} (first line in (2.81)). This parameter may be used again to compute the actual modal coordinate by simply multiplying it by the solution determined as mentioned above (second line in (2.81)).

$$\begin{aligned}&\ddot{Y}'_n + 2\cdot\omega_n\cdot\xi_n\cdot\dot{Y}'_n + \omega_n^2\cdot Y'_n = \ddot{q}_{sJ}(t) \quad \Rightarrow \quad Y'_n \\ &\textit{Final Modal Coordinate}, Y_n \quad \Rightarrow \; Y_n = P_{nJ}\cdot Y'_n\end{aligned} \tag{2.81}$$

As before, the equation of motion under direction *J* for the *n*th degree of freedom may be computed applying the transformation (2.60).

$$q_{n,J}(t) = \sum_{i=1}^{N}\phi_{n,i}\cdot P_{iJ}\cdot Y'_n(t) \tag{2.82}$$

It appears from this expression, that the modal participation factor serves also as a measure of each mode contribution for the response in geometric coordinates. For instance, consider the response of a degree of freedom under *X* direction, in a given MDOF system. It is expected that modes with displacements mainly under *X* direction will contribute more to this response, than other modes having their displacements mainly in other directions.

2.12 Vibration Analysis by the Rayleigh Method

The Rayleigh method is widely used as it provides a simple method of evaluating the natural frequency both for SDOF and MDOF systems.

Basic concepts

The basic concept in this method is the *principle of conservation of energy*. This implies that the energy of a SDOF system, as shown in figure 1, must remain constant if no damping forces, f_c, act to absorb the energy when the system is freely vibrating. The total energy in this case consists of the sum of the kinetic energy of the mass, *T*, and the potential energy of the spring, *V*.

The motion of this system may be assumed harmonic i.e.:

$$q(t) = Z_0 \cdot sin(\omega \cdot t) \tag{2.83}$$

where Z_0 is the amplitude and ω the frequency.

Under these conditions is evident that:

- when the systems is in its neutral position, *q(t)=0*, the force of the spring is *0* and the velocity is maximum, $Z_0 \cdot \omega$. The entire energy of the system is then given by the kinetic energy of the mass:

$$T_{max} = \frac{1}{2} \cdot m \cdot (Z_0 \cdot \omega)^2 \tag{2.84}$$

- when the system is at maximum displacement the velocity of the mass equals *0* which means that the entire energy of the system is the potential energy of the spring:

$$V_{max} = \frac{1}{2} \cdot k \cdot Z_0^2 \tag{2.85}$$

According to the principle of conservation of energy, for the present conditions, the previous expressions must be equal. Thus the same result is established as in (2.10):

$$\begin{aligned} \frac{1}{2} \cdot m \cdot (Z_0 \cdot \omega)^2 = \frac{1}{2} \cdot k \cdot Z_0 \quad \Leftrightarrow \\ \Leftrightarrow \qquad \omega = \sqrt{\frac{k}{m}} \end{aligned} \tag{2.86}$$

Approximate analysis of a general system; Selection of the vibration shape

The main advantage of this method is that it provides a simple procedure to determine a good approximation of the natural frequency of MDOF systems.

Consider a simply supported beam as shown in figure 7.

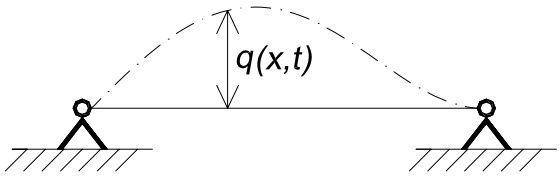

Figure 7 – Simply supported beam with a selected deformed shape possible

This beam may be considered as a MDOF system as it has an infinite number of degrees of freedom. To apply the Rayleigh method one has to assume a deformed shape for the fundamental mode of vibration so that it may be possible to compute the maximum potential and kinetic energy.

This may be achieved writing the deformed shape in terms of a shape function, $\psi(x)$, representing the ratio of the displacement at any point *x* to a reference displacement, *Z(t)*, varying harmonically in time (see figure 7):

$$q(x,t) = \psi(x) \cdot Z(t) \tag{2.87}$$

with $Z(t) = Z_0 \cdot \sin(\omega \cdot t)$.

The previous assumption of the shape function, $\psi(x)$, effectively reduces the beam to a SDOF system as the knowledge of a single function allows the evaluation of the displacement of the entire system.

The flexural strain energy, *V*, of a prismatic beam, as shown in figure 7, is given by the following expression, *EI* being the bending stiffness,

$$V = \frac{1}{2} \cdot \int_0^L EI(x) \cdot \left[\frac{d^2 q(x,t)}{dx^2} \right]^2 dx \tag{2.88}$$

Introducing equation (2.87) into this expression and letting the reference displacement, *Z(t)*, take its maximum value one finds the following expression for the maximum strain energy, V_{max}:

$$V_{\max} = \frac{1}{2} \cdot Z_0^2 \cdot \int_0^L EI(x) \cdot \left[\frac{d^2 \psi(x)}{dx^2} \right]^2 dx \tag{2.89}$$

The kinetic energy of the beam vibrating as assumed in (2.87) is:

$$T = \frac{1}{2} \cdot \int_0^L m(x) \cdot \left[\frac{dq(x,t)}{dt} \right]^2 dx \tag{2.90}$$

where m(x) is the mass per unit length.

Proceeding as above to find the maximum strain energy, one may write the maximum kinetic energy as follows:

$$T_{max} = \frac{1}{2} \cdot Z_0^2 \cdot \omega^2 \int_0^L m(x) \cdot \psi(x)^2 \, dx \tag{2.91}$$

The application of the principle of conservation of energy leads to the following natural vibration frequency:

$$\omega = \sqrt{\frac{\int_0^L EI(x) \cdot \left[\frac{d^2\psi(x)}{dx^2} \right]^2 dx}{\int_0^L m(x) \cdot \psi(x)^2 \, dx}} \tag{2.92}$$

The accuracy of the vibration frequency obtained by the Rayleigh method depends entirely on the shape function assumed, $\psi(x)$. Any shape function satisfying the geometrical boundary conditions may be selected as it represents a possible vibration shape. However, any shape other than the natural vibration shape requires the action of additional external constraints that contribute to stiffen the system and therefore to increase the corresponding frequency. Consequently from the infinity of vibration shapes possible in a general system, the true vibration shape yields the lowest frequency.

A good approximation to the natural frequency / vibration shape may be obtained considering the static performance of the system.

One common assumption is to identity the inertia forces with the *weight* of the masses in the system. The frequency is then evaluated assuming that the vibration shape, $\psi(x)$, is the deflected shape resulting from the application the weight in the direction where the principal vibratory motion is expected to take place. Therefore considering the system in figure 5a) one would assume the weight load being vertical as this is the direction where the vibration motions are expected to take place. In a multi-storey building the vibration shape is mainly due to horizontal displacements of each storey and so the inertia forces should be put in the horizontal direction.

In the following the application of this procedure in determining the natural frequency of a MDOF system with *N* degrees of freedom is explained.

According to (2.87) the displacements for the degree of freedom *n* is given by the expression:

$$q_n(t) = Z_n \cdot sin(\omega \cdot t) \tag{2.93}$$

Here Z_n is the amplitude, which depends on the position of the mass and may be taken as the displacement at the degree of freedom when the system is acted upon by the weight load.

The potential energy is given by the sum of the work of each weight-load, W_n. The maximum potential energy is given by:

$$V_{\max} = \frac{1}{2} \cdot \sum_{i=1}^{N} W_n \cdot Z_n \tag{2.94}$$

The maximum velocity of mass number *n*, may be easily found using equation (2.93). One gets $\dot{q}_{n,\max} = \omega \cdot Z_n$.

Therefore the maximum kinetic energy may be written in the form:

$$T_{\max} = \frac{1}{2} \cdot \sum_{i=1}^{N} \frac{W_n}{g} \cdot \omega_n^2 \cdot Z_n^2 \tag{2.95}$$

Thus the frequency in a MDOF with *N* degrees of freedom determined by equating the maximum values for the strain and kinetic energies, respectively, is:

$$\omega = \sqrt{g \cdot \frac{\sum_{i=1}^{N} W_n \cdot Z_n}{\sum_{i=1}^{N} W_n \cdot Z_n^2}} \tag{2.96}$$

3. Seismic Analysis by Response Spectra

Response spectrum analysis is perhaps the most common method used in design to evaluate the maximum structural response due to the seismic action. This is a linear approximate method based on modal analysis and on a response spectrum definition. According to the analogy between SDOF and MDOF systems, the maximum modal response of the *n*th mode, Y_n^{max} , is the same as for a SDOF system having $\omega = \omega_n$ and $\xi = \xi_n$ (see equation (2.75))

It should be emphasized that this procedure only leads to the maximum response, instead of fully describing the response. This saves up a lot of calculation effort with evident consequences in the time consumed and CPU requirements. The maximum response is established for each mode by means of the adequate response spectrum. Therefore the response spectrum analysis is often considered to be the most attractive method for the seismic design of a given structural system.

3.1 Response Spectrum Concept

To explain the response spectrum concept, one considers a SDOF system submitted to an external action that may be either an applied force or a support displacement. The procedures used to formulate and solve the equation of motion, $q(t)$, and therefore to achieve the time dependent response of the referred SDOF system, were already discussed in paragraphs 2.1 to 2.5. For the response spectrum definition, it is necessary to evaluate the value of the maximum response, which may be easily determined once its equation of motion, $q(t)$, is fully known.

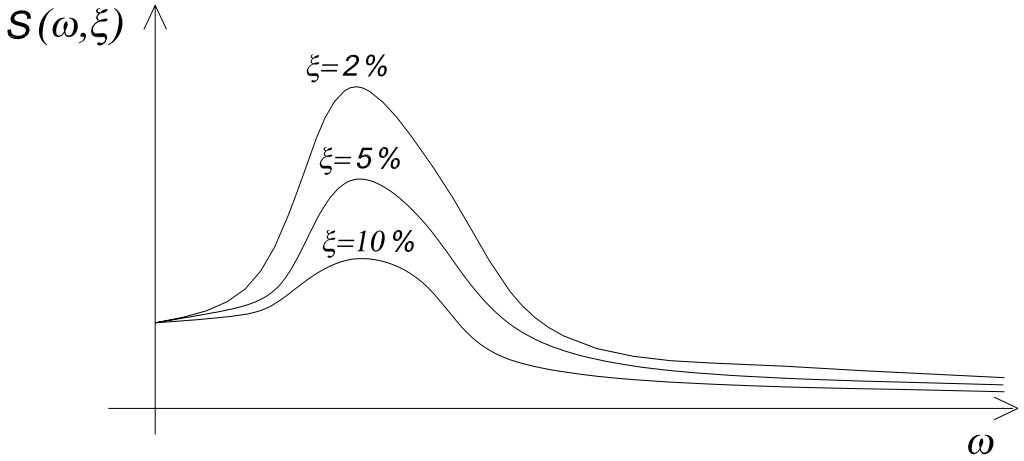

Figure 8 – Typical representation of response spectrum

If the procedure of determining the maximum response is repeated for a sufficient range of SDOF systems, with a specified critical damping ratio, ξ, and for different natural vibration frequencies, ω, submitted to the same external action, it is possible to define a function and represent it in a diagram similar to the one shown in figure 8.

This diagram is generally known as a response spectrum, $S(\omega,\xi)$. Usually it is represented with the *x*-axis being the natural vibration frequencies or periods of vibration[8] of the SDOF and the *y*-axis being the corresponding maximum response values. Generally, in the same graph different response spectra, corresponding to the same action and to different damping ratios usually found in common structures (2%, 5% and 10%) are shown as in figure 8.

Figure 8 represents a typical relative displacement response spectrum, $S_d(\omega,\xi)$, for values of critical damping ratio, ξ, usually found in common structural systems. The meaning of the relative displacement, *q**, was already discussed in paragraph 2.5. It is worth to analyse the evolution of the response spectrum function:

1) For low values of frequency, close to zero, one may see that the maximum value for the relative displacement tends to a certain value, which is the support displacement, q_s. This is easily explained if one remembers the concept of the natural vibration frequency, ω, in a SDOF system, described by expression (2.10). In fact a SDOF with a low value of ω is very flexible and behaves as shown in figure 9 when submitted to a support displacement.

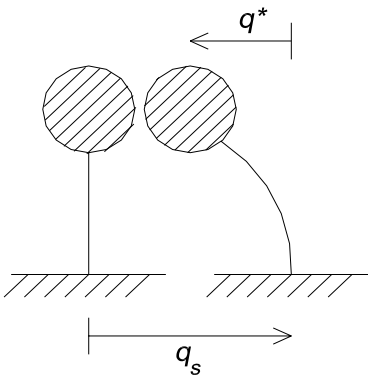

Figure 9

2) After a certain value of frequency, the relative displacement tends to zero. In fact high values of frequency correspond to a very stiff system. The response motion will then be as shown in figure 10 – the relative displacements, *q**, tend to zero.

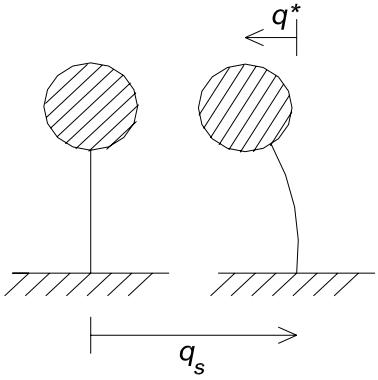

Figure 10

It should be noted that the maximum responses, $S(\omega,\xi)$ may be presented in every desired form, i.e. for displacements, $S_d(\omega,\xi)$, velocities, $S_v(\omega,\xi)$, and accelerations, $S_a(\omega,\xi)$, or even in the form of internal forces or bending moments in a given point of the SDOF system.

[8] The period *T*, in seconds, is the inverse of the cyclic frequency in Hz (cycles per second)

The available response spectra used for design purpose, in most of the Seismic Design codes, are defined by means of an accelerogram representing a typical earthquake in the region of the structure.

N.B.: An accelerogram is a record of the ground accelerations either measured in a certain place or generated artificially.

3.2 Response Spectrum Analysis Applied to MDOF Systems

It was concluded in chapter 2.11 that the equation of motion for the *n*th degree of freedom under a support excitation in direction *J* for a given MDOF system may be written as in (3.1):

$$q_{n,J}(t) = \sum_{i=1}^{N} \phi_{n,i} \cdot P_{iJ} \cdot Y'_n(t) \tag{3.1}$$

As mentioned, the term P_{iJ} may be omitted, and so the modal coordinate, $Y'_n(t)$, may be found using to the analogy between equations (2.80) and (2.22) for MDOF and SDOF systems, respectively.

For direction *J*, the maximum value for the modal coordinate in terms of displacements, $Y'_{n,\max}$, may be easily achieved if the displacement response spectrum, $S_d(\omega,\xi)$, is available. Instead of solving mathematically an expression in the form of (2.80), $Y'_{n,\max}$ is established from the response spectrum, $S_d(\omega_n,\xi_n)$, for the SDOF system with both the same natural vibration frequency, ω_n and critical damping ratio, ξ_n. The procedure is illustrated in figure 11.

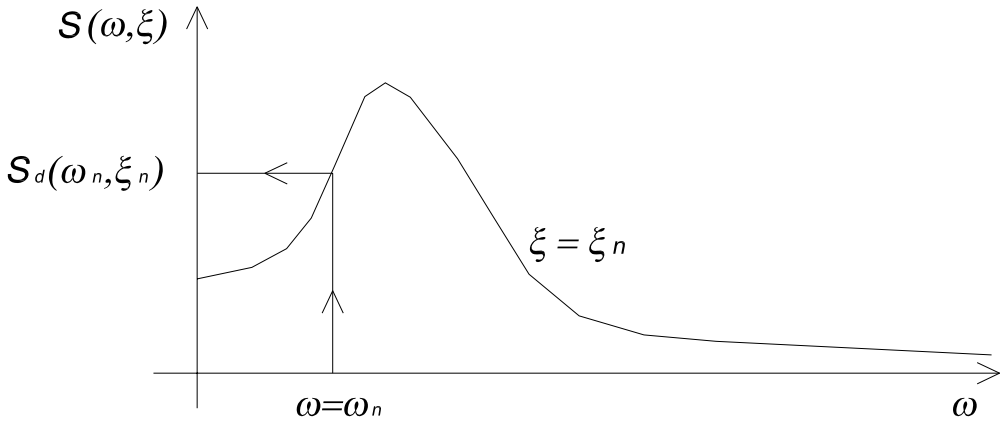

Figure 11

After establishing the maximum value for the modal coordinate, $Y'_{n,\max} \doteq S_d$, the modal participation factor is recovered as:

$$Y_{n,max} \doteq P_{iJ} \cdot S_{d,J}(\omega_n,\xi_n) \tag{3.2}$$

In the same way one may calculate the maximum response in terms of accelerations, $\ddot{Y}_{n,\max}$, or velocities, $\dot{Y}_{n,\max}$, if the corresponding spectra, $S_a(\omega)$ or $S_v(\omega)$ are accessible[9].

$$\ddot{Y}_{n,max} \doteq P_{iJ} \cdot S_{a,J}(\omega_n, \xi_n) \tag{3.3}$$

$$\dot{Y}_{n,max} \doteq P_{iJ} \cdot S_{v,J}(\omega_n, \xi_n) \tag{3.4}$$

We now discuss the problem of establishing a reasonable value for the global maximum response of the system. The assumption behind the reasoning expressed in (3.1), i.e. to sum the maximum values of each modal coordinate, $Y_{n,max}$, certainly will correspond to an upper limit of the global response with a low probability of occurrence, since is very unlikely for the maximum modal responses to happen simultaneously. In fact this is the main disadvantage of the response spectra analyses: The result provided is a set of extreme values that don't take place at the same time and therefore do not correspond to an equilibrium state. Thus this method can't provide information on the failure mode of the structure, which is an important information from the engineering point of view.

To minimize these disadvantages it is necessary to combine the modal responses. There are several ways of carrying out this and it is out of the purpose of the present text to discuss them. Therefore only two methods are presented. It should be mentioned that there is some controversy about which method leads to better results. In the design codes, usually the first method to be discussed below is suggested. However is up to the designer to choose more accurate procedures of combining the modal response if the SRSS method can't be applied.

1) SRSS (Square Root of Sum of Squares)

This is one of the most frequently used modal combination methods. According to this rule the maximum response in terms of a given parameter, *G*, (displacements, velocities, accelerations or even internal forces) may be estimated through the square root of the sum of the *m* modal response squares, $(G_n)^2$, contributing to the global response, i.e.

$$G \approx \sqrt{\sum_{n=1}^{m} (G_n)^2} \tag{3.5}$$

This method usually gives good results if the modal frequencies of the modes contributing for the global response are sufficiently separated to each other. Otherwise another method, such as the one following, will be more adequate.

[9] Alternatively this may be done by means of the so-called *pseudo-response-spectra*. These are determined remembering that each vibration mode will have an expression in the form of (2.42) for the corresponding equation of motion. Therefore one has $S_v(\omega) \doteq \omega \cdot S_d(\omega)$ and $S_a(\omega) \doteq \omega^2 \cdot S_d(\omega)$.

2) CQC (Complete Quadratic Combination)

The reason why this method is more effective in evaluating the maximum response when the modal frequencies are close to each other is due to the fact that it considers the correlation between modal responses, whereas the SRSS method considers these to be independent. In fact if two vibration modes have close frequencies their contribution to the global response is not independent. Usually this method is used if $\omega_{n+1}/\omega_n \leq 1.5$. The correlation between modes *i* and *n* is estimated using the parameter, ρ_{in} , given by the following expression:

$$\rho_{in} = \frac{8 \cdot \xi^2 \cdot (1+\beta_{in}) \cdot \beta_{in}^{3/2}}{(1-\beta_{in}^2)^2 + 4 \cdot \xi^2 \cdot \beta_{in} \cdot (1+\beta_{in})^2} \tag{3.6}$$

The parameter β_{in} is $\beta_{in} = \frac{\omega_i}{\omega_n}$.

The global response is achieved applying the following expression.

$$G \approx \sqrt{\sum_{n=1}^{m}\sum_{i=1}^{m} \rho_{in} \cdot G_i \cdot G_n} \tag{3.7}$$

3.3 Ductile Behaviour Consideration

As may be understood by the discussion so far, earthquake analysis by response spectra is based on the assumption that the system behaves linearly. This means that even for the maximum response situation the internal forces on the different structural elements of the system are assumed to be proportional to the displacements achieved.

However this hypothesis is far from reality for structural materials as reinforced concrete or steel. For instance, a sketch of the stress-strain curve for steel, in figure 12, shows that this material will roughly behave linearly until yielding and thereafter non-linearly until failure. The symbols ε_y and ε_u stand for yielding and ultimate strains, respectively.

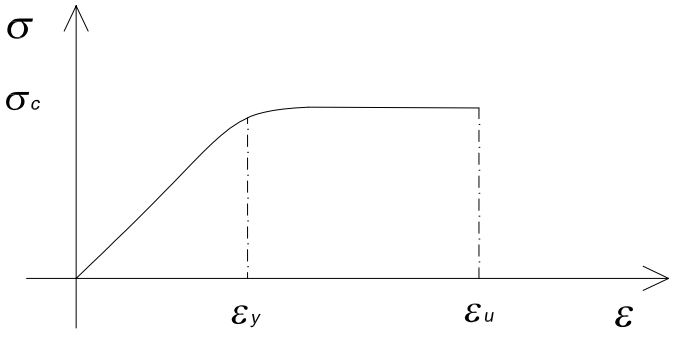

Figure 12 – Typical stress-strain curve for steel in uniaxial tension or compression

The capacity of the material to absorb deformations in a stabilized way is called ductility. One way of measuring ductility is the ratio of ultimate deformation to the yielding deformation. The larger this value the more ability of the material to dissipate energy after yielding, and therefore the more ductile.

The seismic design criteria consider that a structure submitted to an extreme earthquake should be prevented from collapse but significant damage is expected. Therefore this type of action must be included among the design load conditions for the Ultimate Limit State design. Under these conditions, yielding is expected which will lead to inelastic response of the structure.

Assuming that the deflections, δ, produced by a given earthquake are essentially the same whether the structure behaves linearly or yields significantly, one can utilize the non-linear behaviour and design structures for less values of stresses, σ, or internal forces, F. This idea is illustrated in figure 13.

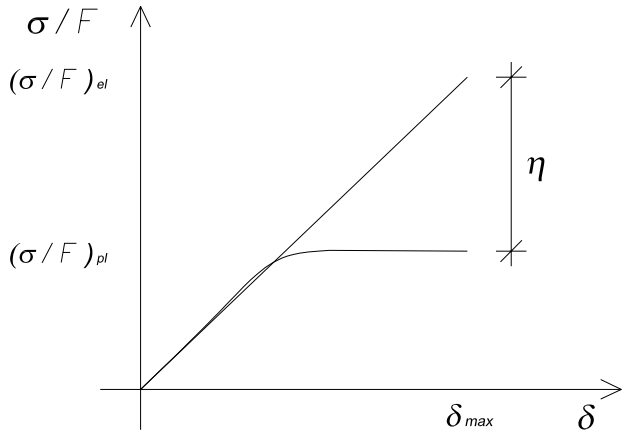

Figure 13

Therefore if the response spectra method is used to design a structural system, the stresses / internal forces corresponding to the maximum deformations previously achieved may be reduced to take into account the yielding of the material. This is done by means of the coefficient, η, called *the reduction factor* or *behaviour coefficient* the physical meaning of which is shown in figure 13.

The determination of this coefficient is also a matter of controversy. Usually, the value given for the behaviour coefficient is much less than the real one as the elastic response is reduced using further reduction coefficients (see chapter 6). However, it is accepted that in order to maximize the non-linear behaviour of the system and thus its behaviour coefficient, it is desirable to design it in a redundant way i.e. with a sufficient number of plastic hinges allowed before collapse.

It should be stated that ductility does not depend only on the material characteristics but also on the system and the direction of loading. Consider, for instance, the MDOF system in figure 5 b). The horizontal motion of the mass will induce bending moments on the column whereas the vertical motion of the mass will lead to a compression /

tension. For the first situation the moment-rotation curve will show that the element has capacity to absorb deformations after yielding and so ductile behaviour may be assumed. On the other hand, the axial force – axial deformation diagram often show brittle behaviour and so $\eta = 1$ is usually adopted. This is the reason why in most of the analyses, for vertical seismic action, the reduction factor is taken as unity.

4. Seismic Response by Time-History Analysis

Time-History analysis is a step-by-step procedure where the loading and the response history are evaluated at successive time increments, Δt – *steps*. During each step the response is evaluated from the initial conditions existing at the beginning of the step (displacements and velocities) and the loading history in the interval. With this method the non-linear behaviour may be easily considered by changing the structural properties (e.g. stiffness, *k*) from one step to the next. Therefore this method is one of the most effective for the solution of non-linear response, among the many methods available. Nevertheless, in the present text, a linear time history analysis is adopted i.e. the structural properties are assumed to remain constant during the entire loading history and further it is assumed that the structure behaves linearly. As a consequence the mode superposition method, already discussed in chapter 2, may be applied.

4.1 Response of a SDOF System to General Dynamic Loading; Duhamel's Integral

The equilibrium equation for a given general dynamic loading, *p(t)*, may be expressed in the same form as (2.22) for a damped SDOF system, i.e.:

$$\ddot{q}(t) + 2 \cdot \xi \cdot \omega \cdot \dot{q}(t) + \omega^2 \cdot q(t) = \frac{p(t)}{m} \tag{2.22}$$

It should be noted that both the response, *q(t)*, and the dynamical loading, *p(t)*, depend on time. The purpose of Duhamel's integral is to achieve the response at any time, *t*, due to load applied at another time τ.

The response to general dynamic loading of a SDOF system subjected to initial conditions q_0 and $\dot{q}_0$ is deduced considering first the corresponding free vibration response as in equation (2.20).

$$q(t) = e^{-\xi \cdot \omega \cdot t}\left[q_0 \cdot cos(\omega_d \cdot t) + \frac{\dot{q}_0 + q_0 \cdot \xi \cdot \omega}{\omega_d} \cdot sin(\omega_d \cdot t) \right] \tag{2.20}$$

If the starting time is different from *0*, the above expression may be written in a general form introducing τ as the time corresponding to the initial conditions:

$$q(t - \tau) = e^{-\xi \cdot \omega \cdot (t - \tau)}\left[q(\tau) \cdot cos(\omega_d \cdot (t - \tau)) + \frac{\dot{q}(\tau) + q(\tau) \cdot \xi \cdot \omega}{\omega_d} \cdot sin(\omega_d \cdot (t - \tau)) \right] \tag{4.1}$$

Now we consider the same SDOF system acted upon by a load $p(\tau)$. This load induces into the system a velocity variation, $\Delta\dot{q}$, in the interval $\Delta\tau$ given by the impulse-momentum relationship:

$$m \cdot \Delta\dot{q} = \int p(\tau)\, d\tau \tag{4.2}$$

The second term in this equation represents the area of the plot $p(\tau)$ in the time interval $\Delta\tau$. For a differential time interval, $d\tau$, this area is simply $p(\tau)d\tau$, which allows to re-write equation (4.2) as follows:

$$m \cdot d\dot{q}(\tau) = p(\tau)\, d\tau \tag{4.3}$$

Using the previous relation and noticing that the response after the termination of the short duration impulse, $p(\tau)\, d\tau$, is a free vibration motion subjected to an initial velocity, $d\dot{q}(\tau)$, one may write the differential response, *dq(t)*, as follows, *for t>τ*:

$$dq(t) = e^{-\xi\cdot\omega\cdot(t-\tau)}\left[\frac{p(\tau)\cdot d\tau}{m\cdot\omega_d}\cdot sin\left(\omega_d\cdot(t-\tau)\right)\right] \tag{4.4}$$

The entire loading history may be considered to consist of a succession of such short impulses, each producing its own differential response according to the expression above. Because the system is assumed to be linear, the total response may be established by summing all the differential responses developed during the loading history. This is the same as saying that the response at time *t* is given by the integral of the differential displacements since time *t=0* until time *t*., i.e.:

$$q(t) = \frac{1}{m\cdot\omega_d}\cdot\int_0^t p(\tau)\cdot e^{-\xi\cdot\omega\cdot(t-\tau)}\cdot sin\left(\omega_d(t-\tau)\right) d\tau \tag{4.5}$$

This result is known as *Duhamel's Integral* and is one of the most important results in Structural Dynamics as it may be used to express the response of any damped SDOF system subjected to any form of dynamical loading, $p(\tau)$. There are several procedures to evaluate this integral and it is out of the purpose of this text to discuss them here.[10]

To take into account initial conditions, the free damped vibration response must be added to the solution, which leads to the result:

$$\begin{aligned} q(t) = e^{-\xi\cdot\omega\cdot t}&\left[q_0\cdot cos\left(\omega_d\cdot t\right) + \frac{\dot{q}_0 + q_0\cdot\xi\cdot\omega}{\omega_d}\cdot sin\left(\omega_d\cdot t\right)\right] + \\ &+ \frac{1}{m\cdot\omega_d}\cdot\int_0^t p(\tau)\cdot e^{-\xi\cdot\omega\cdot(t-\tau)}\cdot sin\left(\omega_d(t-\tau)\right) d\tau \end{aligned} \tag{4.6}$$

[10] References 1, chapter 7, and reference 2, section 4, provide useful information about the evaluation of the Duhamel Integral for SDOF systems.

As one may notice the general response in the form (4.6) for damped SDOF systems is composed by two terms with the same nature as discussed in paragraph 2.4. The first term reflects only the influence of the initial conditions and the second term corresponds to the loading effect on the structural response.

4.2 Linear Time History Analysis for MDOF Systems

It may be inferred from the discussion held in paragraphs 2.6 to 2.11, that the solution given by the Duhamel Integral may be used to determine the modal coordinates of a given MDOF system submitted to general dynamic loading. The mode superposition method is then used to determine the global response of the system.

The determination of the modal coordinates of a given MDOF systems, $Y_n(t)$, is accomplished from equation (2.72) in which the vector $\{p(t)\}$ represents the general dynamic loading applied in the corresponding degrees of freedom.

$$\ddot{Y}_n(t) + 2 \cdot \omega_n \cdot \xi_n \cdot \dot{Y}_n(t) + \omega_n^2 \cdot Y_n(t) = \phi_n^T \cdot \{p(t)\} \tag{4.7}$$

The modal coordinate $Y_n(t)$, has the same form as (4.5), assuming that the system starts from rest, with $\xi = \xi_n$ and $\omega = \omega_n$, i.e.:

$$Y_n(t) = \frac{e^{-\xi_n \cdot \omega_n \cdot t}}{\omega_{d,n}} \cdot \sum_{i=1}^{N} \int_0^t e^{\xi_n \cdot \omega_n \cdot \tau} \cdot \phi_{in} \cdot p_i(\tau) \cdot sin\left(\omega_{d,n} \cdot (t - \tau)\right) d\tau \tag{4.8}$$

Once this procedure is done for all normal coordinates, one applies the expression (2.60) to obtain the time dependent equation of motion for each degree of freedom in geometric coordinates. This will lead to the global response of the system at any desired time *t*.

If the system is submitted to initial conditions different from zero, then it is obvious that equation (4.8) would have to be written in the form of (4.6). For this case one would have to compute the modal initial conditions $q_{0,n}$ and $\dot{q}_{0,n}$ as expressed in (2.61) considering the vectors $\{q_0\}$ and $\{\dot{q}_0\}$.

It should be noticed that, in order to obtain the equation of motion for a given degree of freedom at a time *t* in a MDOF system with *N* degrees of freedom, it is required to solve the set of *N* equations as (4.8). To obtain the global response of the system it is necessary to compute the equation of motion for the *N* degrees of freedom. This is done by means of expression (2.60). Therefore one may conclude that to establish the deformed shape of a structure at a certain time *t*, *N*x*N* equations in the form of (4.8) must be solved. If one wants to represent the time history of the displacements, then a set of time intervals must be established taking into account the desired accuracy of the time history representation. If the time history has *m* time intervals then it is obvious that *mxNxN* equations in the form of (4.8) must be solved. In most

cases less than *N* modes are considered since, the modes corresponding to high frequencies have a small contribution for the response of the structure.

Thus, it may be concluded, that the decision about the number of degrees of freedom and the desired accuracy for the time history representation affect directly the number of calculations to accomplish and therefore must be chosen carefully taking into account the time consuming and the CPU requirements to proceed a time history analysis. However, for some structures or certain types of analysis the number of degrees of freedom may be very high, which makes the application of this method impracticable. This is actually one of the main disadvantages of the method.

4.3 Time History Analysis for Earthquakes

As mentioned before, an earthquake action is considered as a base motion computed on the basis of the support acceleration. Thus all the results in paragraph 2.5 and 2.11 may be applied.

Separating the support acceleration vector, $\ddot{q}_s(t)$, in its three components, along the axes *X*, *Y* and *Z*, we have for each degree of freedom a dynamic load given by the product of the mass, *m*, and the corresponding acceleration value, $\ddot{q}_{sJ}(t)$.

As stated in paragraph 2.11, the definition of the modal coordinates $Y_n(t)$ may be done for each direction separately, using the mode superposition approach and the assumed linear behaviour of the system. If expression (2.80) is used, the equation of motion for the *n*th mode under direction *J* is the following:

$$\ddot{Y}_n(t) + 2 \cdot \omega_n \cdot \xi_n \cdot \dot{Y}_n(t) + \omega_n^2 \cdot Y_n(t) = P_{nJ} \cdot \ddot{q}_{sJ}(t) \tag{4.9}$$

Remembering the expression of the modal participation factor, P_{nJ}, it is obvious that the second term in (4.9) may be written as:

$$P_{nJ} \cdot \ddot{q}_{sJ}(t) = \phi_n^T \cdot [M] \cdot \{1_J\} \cdot \ddot{q}_{sJ}(t) \tag{4.10}$$

The analogy between expression (4.9) and (4.7) is evident expressing the load vector $\{p(t)\}$ as:

$$\{p(t)\} \doteq [M] \cdot \{1_J\} \cdot \ddot{q}_{sJ}(t) \tag{4.11}$$

A solution is achieved by substituting into equation (4.8) the term $\{p(t)\}$ by $[M] \cdot \{1_J\} \cdot \ddot{q}_{sJ}(t)$ which leads to:

$$Y_n(t) = \frac{e^{-\xi_n \cdot \omega_n \cdot t}}{\omega_{d,n}} \cdot \int_0^t e^{\xi_n \cdot \omega_n \cdot \tau} \cdot P_{nJ} \cdot \ddot{q}_{sJ}(\tau) \cdot sin\left(\omega_{d,n} \cdot (t - \tau)\right) d\tau \tag{4.12}$$

The problem now consists in solving this expression above for each modal coordinate. One of the most common techniques is to assume the load subdivided into a sequence of time intervals, *steps*, in which the modal coordinates, $Y_n(t)$, are

calculated. This procedure is called *the step-by-step integration method* and next we shall briefly describe one of the many different ways to solve it.

Step-by-step integration method with linear variation of the load

In order to perform a time history analysis of a given structure, normally, the designer uses an accelerogram of a certain earthquake considered to be a typical seismic action. As previously stated an accelerogram may be a record of the ground accelerations measured in a certain place during the period of an earthquake. A complete accelerogram contains the record of the acceleration for the three directions corresponding to the three cartesian axes, *X*, *Y* and *Z*, and therefore making automatically available to the designer the values of $\ddot{q}_{sX}(t)$, $\ddot{q}_{sY}(t)$ and $\ddot{q}_{sZ}(t)$.

According to the desired accuracy of the time history analysis, the designer decides the number of time intervals, Δt, in which each acceleration component should be divided. The acceleration is assumed to vary linearly within the referred interval between the initial value, $\ddot{q}_{sJ,0}(\tau)$, and the final value, $\ddot{q}_{sJ}(\tau+\Delta t)$, i.e.:

$$\ddot{q}_{sJ}(\tau) = \ddot{q}_{sJ,0}(\tau) + \frac{\ddot{q}_{sJ}(\tau+\Delta t) - \ddot{q}_{sJ,0}(\tau)}{\Delta\tau}\cdot\tau \tag{4.13}$$

Thus, equation (4.12) for the modal coordinate, $Y_n(\Delta t)$, becomes:

$$Y_n(\Delta t) = \frac{e^{-\xi_n\cdot\omega_n\cdot\Delta t}}{\omega_{d,n}}\cdot P_{nJ}\cdot\int_0^{\Delta t} e^{\xi_n\cdot\omega_n\cdot\tau}\cdot\left(\ddot{q}_{sJ,0}(\tau)+\frac{\ddot{q}_{sJ}(\tau+\Delta t)-\ddot{q}_{sJ,0}(\tau)}{\Delta\tau}\cdot\tau\right)\cdot sin\left(\omega_{d,n}\cdot(t-\tau)\right)d\tau \tag{4.14}$$

It should be noted that this expression is exact for the first time interval assuming that the system is at rest until the load is applied. For the next time intervals, Δt_i, regarding the continuity of the response, the initial conditions, $Y_{n,i-1}$ and $\dot{Y}_{n,i-1}$ must be determined. These parameters are achieved computing the response at the end of the previous time interval, Δt_{i-1}, in terms of displacements and velocities. Therefore at the time $i\cdot\Delta t$ the response for the modal coordinate *n* is of the same form as (4.6), i.e.:

$$\begin{aligned} Y_n(i\cdot\Delta t) = {} & e^{-\xi\cdot\omega_n\cdot\Delta t}\left[Y_{n,i-1}\cdot cos(\omega_{d,n}\cdot t)+\frac{\dot{Y}_{n,i-1}+Y_{n,i-1}\cdot\xi\cdot\omega_n}{\omega_{d,n}}\cdot sin(\omega_{d,n}\cdot t)\right]+ \\ & +\frac{e^{-\xi_n\cdot\omega_n\cdot\Delta t}}{\omega_{d,n}}\cdot P_{nJ}\cdot\int_0^{\Delta t} e^{\xi_n\cdot\omega_n\cdot\tau}\cdot\left(\ddot{q}_{sJ,0}(\tau)+\frac{\ddot{q}_{sJ}(\tau+\Delta t)-\ddot{q}_{sJ,0}(\tau)}{\Delta\tau}\cdot\tau\right)\cdot sin\left(\omega_{d,n}\cdot(t-\tau)\right)d\tau \end{aligned} \tag{4.15}$$

Once all the modal coordinates have been determined for the time $i\cdot\Delta t$, it is possible to compute the corresponding global response in terms of geometric coordinates using superposition. The repetition of this procedure for each time interval leads to the time history response of the structure.

5. Equivalent Static Method

This method is perhaps the simplest procedure at disposal for a structural engineer to perform an earthquake analysis and achieve reasonable results. It is prescribed in any relevant code for earthquake analysis and is widely used especially for buildings and other common structures meeting certain regularity conditions.

The method is also called *The Lateral Forces Method* as the effects of an earthquake are assumed to be the same as the ones resulting from the statical transverse loadings.

As discussed before, in the Rayleigh method, an inertia loading provides a good approximation to the natural vibration shape of the structure. If the structural response is not significantly affected by contributions from higher modes of vibration it is reasonable to assume that with an appropriate set of inertia forces one may achieve a good approximation for the response. This is the basic concept of the *Equivalent Static Method*.

Each code presents its own procedure to compute and to distribute the static equivalent forces in order to achieve the earthquake effects on the structure[11]. Usually an expression is defined to prescribe the minimum lateral seismic force, also designated the base *shear force*.

One usual requirement for the structure regarding the application of this method is that the natural vibration period of the structure should be limited by a maximum value, which leads to a certain minimum value of frequency/stiffness. This is due to the fact that often the response is mainly controlled by the first mode of vibration. Thus, imposing a minimum value of frequency the higher modes contribution may be neglected.

The structure to be analysed by the equivalent static method should respect certain criteria regarding its geometrical regularity and stiffness distribution such as[12]:

- All lateral load resisting elements (such as columns or walls) should run from the base to the top without any interruption:
- Mass and lateral stiffness should not change abruptly from the base to the top;
- Geometrical asymmetries in height or in plan due to setbacks should not exceed certain values;

[11] Regarding the determination and distribution of the static equivalent forces in a given structure, the chapters 23 and 24 at reference 1 and the section 4.3.3.2 in reference 3 are recommended.

[12] A complete set of requirements of this type is presented, for example, in Reference 3 at section 4.3.3.2.1.

6. Case Study

The present chapter presents seismic analyses of a bridge, similar to one designed for the High Speed Transportation System in Taiwan, using the methods discussed before.

6.1 Structural Model of the Bridge

A sketch of the bridge is shown in figure 14.

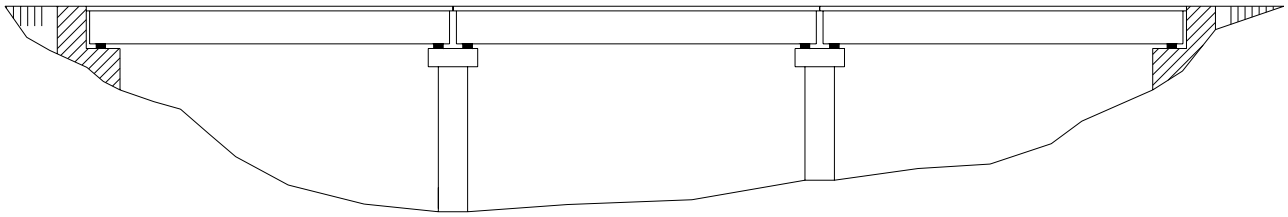

Figure 14

The bridge is a three-span bridge with two rail tracks. Each span has a length 40m and a 13m width. The cross-section is a box girder. The alignment of the main span axis is straight. The piers are 15.80m and 12.35m tall and both are rigidly connected to a shear tap element at the top. The shear tap element is a concrete box with 2m height and of length 5.4m for each side.

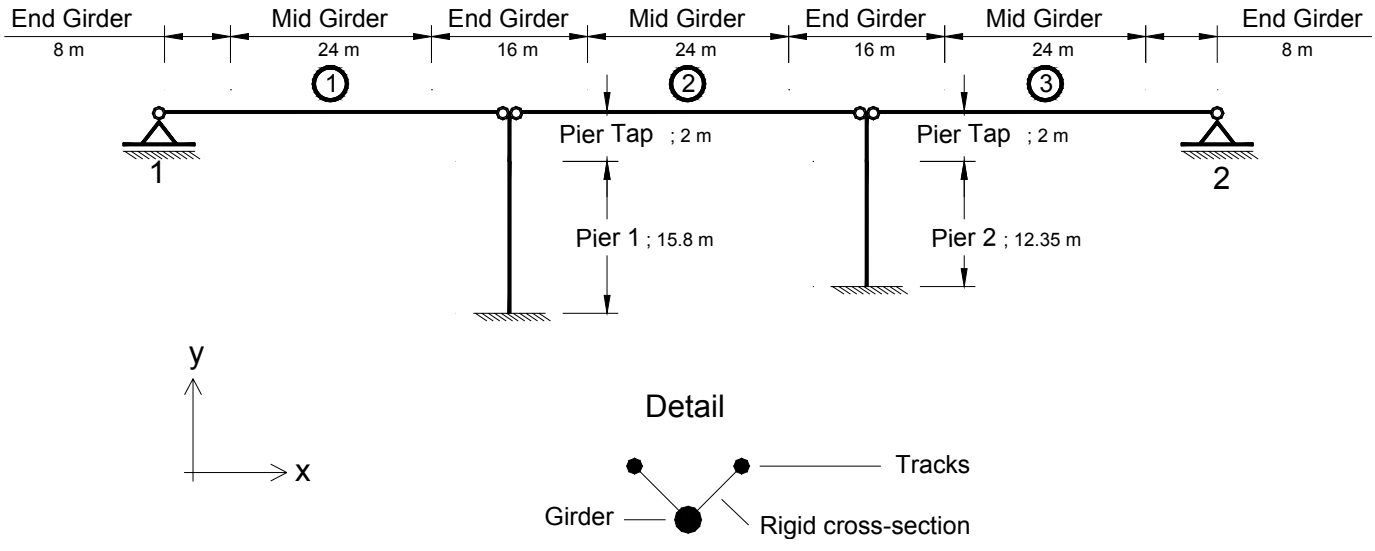

Figure 15 – Structural model (See table 1 for detailed information about cross section properties)

The following assumptions are made for the structural model:

i. The three spans are independent and simply supported at the abutments and shear taps;
ii. The pier supports are assumed to be fixed;
iii. Both abutments allow rotations perpendicular to the bridge plane and restrain all the others;
iv. The abutments (see figure 15) allow translation in the same direction as the main span axis;
v. To take into account the torsional effects due to train loads, the tracks are assumed to be connected to the girder centroid through weightless rigid members (see Detail in figure 15);
vi. Cracked column section with effective flexural rigidity, $(EI)_e$, equal to ½ EI is used.

N.B.: The support system assumed for the piers and abutments is too much on the conservative side. In fact it would be more realistic to admit spring systems to simulate it. However the procedure adopted is considered adequate for the present purpose.

The global axes X and Y are shown in figure 15. The axis Z is defined applying the right-hand rule. The local coordinate system coincides with the global coordinate system for horizontal members. For vertical members the local coordinate system is achieved applying a positive rotation of 90º on the global coordinate system.

Three types of loads are considered:

- Self Weight – the weight of the entire structure which is carrying the loads;
- Superimposed dead load on the span – 200 kN/m in vertical direction which includes the weight of the components other than the main structure stated above;
- One train live load – the weight of a train occupying one track. It is computed as shown in figure 16.

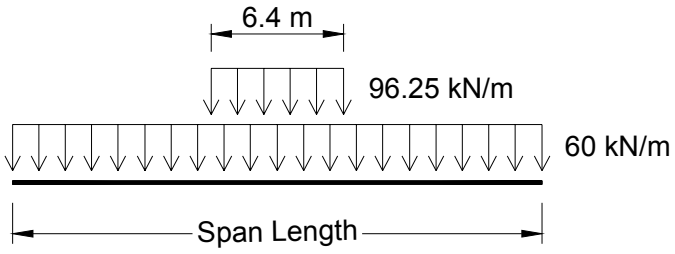

Figure 16 – One train live load

The geometrical parameters of each cross-section shown in Figure 15 are summarized in Table 1.

Table 1 – Geometrical properties of the cross-sections

	A (m^2)	I_{xy} (m^4)	I_{yy} (m^4)	I_{zz} (m^4)	e_y (m)
End Girder	18.7	68.6	109	47.6	-0.53
Mid Girder	8.82	31.9	80.7	20.2	-0.34
Rigid cross-section	1000	1000	1000	1000	0
Tracks	$7.7x10^{-3}$	0.1	0.1	0.1	0
Pier Tap	29.2	120	70.9	70.9	0
Pier	11.5	16.6	12.4	9.83	0

Here:

- A, Cross section area;
- I_{xy}, Torsional moment of inertia;
- I_{yy}, Moment of inertia about local axis y;
- I_{zz}, Moment of inertia about local axis z;
- e_y, local coordinate *y* of shear centre with respect to centroid.

Finally, the material assigned for all the sections is concrete of class *C25/30*. Exceptions for the Rigid cross-section and Pier cross-sections are made considering assumptions vi. and vii., respectively. Therefore no mass density is considered for the concrete assigned for the Rigid cross-section and the Young's Modulus, *E*, is reduced to half the standard value for the Pier cross-section.

6.2 Frequencies and Vibration Mode Shape Determination for the Bridge

The first step to accomplish a dynamical analysis is to *model* the structure as a MDOF system. This means to define the degrees of freedom of the structure. The model definition must represent the real behaviour of the system and plays a fundamental role in the accuracy of the results.

Regarding the geometry of the bridge, the use of uni-axial finite-elements, called members, for all elements (piers, spans or pier tap's) less than 4m long is considered adequate. The drawings A.1 in the Appendix represent the identification of the members and joints adopted in this study

The establishment of the degrees of freedom is done according to the mass distribution and the static loads applied:

- Half of the mass of each member is considered to be concentrated in the nearest joint.
- The sum of the loads applied on each member is concentrated at the middle and "transformed" to a mass dividing by the acceleration of gravity, 9.81 m/s^2.

Thus it is possible to define the mass properties of the structure assuming that the entire mass is concentrated at the nodes at which the translational displacements are specified. This procedure leads to a lumped-mass matrix with null off-diagonal terms and it represents the simplest form of defining the mass properties of a given structure.

In this study 640 degrees of freedom were computed.

The procedures leading to the definition of the stiffness matrix, *[K]*, may be found in any publication about finite-elements and it is out of the purpose to expose them here.

Once the mass and stiffness matrix are computed, each frequency and the corresponding vibration mode shape of the system may be determined using equations (2.44) and (2.43). As one may remember there will be as many modes as degrees of freedom. This means that the above procedure will be repeated successively as many times as the number of the degrees of freedom to achieve all the mode frequencies and vibration shapes.

For the present simplified model, the computation of the 639 frequencies and vibration mode shapes considered does not represent a significant computational effort, regarding the automatic calculation systems available nowadays. More accuracy in the results means bigger refinement of the model, which leads to more degrees of freedom and therefore larger calculation requirements to solve the eigen-value problem.

One of the most common ways to overcome this situation is the *mass participating criterion*. Under this criterion, the response determined by considering only a few modes is a good approximation as long as the mass participating in it exceeds a certain value. Of course, the larger this value the more accurate the results. Usually this value should be bigger than 70%

For this study it is decided to use the first 125 modes, ordered by ascending frequency values. Generally the modes with lower frequencies contribute more for the global response. Table 2 shows, for each direction, the mass participation in terms of percentage of all the mass of the system.

Table 2 – Total mass participation factors for the first 125 modes

	Transverse direction	*Longitudinal direction*	*Vertical direction*
Mass Participation %	97.8	99.89	99.30

As it may be seen, with only 20% (125/640) of the modes, practically all the mass participates in the response. According to the mass participation criterion, the response results determined considering only 20% of the modes are practically the same as considering all the modes, with an evident decrease of the time consumed to perform the calculations.

In the Appendix one may find the results for the eigen-value problem solution. Table A.2.1 summarizes the frequencies / period and each mass participation factor for each mode in the three directions. The following figures refer to the deformed shape of the first three modes, each one with the corresponding displacements in one predominant direction.

Finally, it is worth to compare the results for the first mode shape and frequency given by the eigen-value solution with the solution provided by the application of the Rayleigh method. As one may see in table A.2.1 the solution of the eigen-value problem leads to a frequency of 1.11 Hz for the first mode. The application of the Rayleigh method assumes that the first mode shape will have displacements mainly in the longitudinal direction. Therefore the weight load is applied on this direction in order to compute the natural frequency as in (2.96). The result is 1.53 Hz. As expected, is an upper value of the real frequency. However this is considered to be a good approximation if one compares the figures in Appendix A.2 of the first vibration mode shape given by the eigen-value problem solution with the one given by the Rayleigh method.

6.3 Response Spectrum Analysis of the Bridge

Once the modal frequencies and the vibration mode shapes are computed, a response spectrum analysis may be done.

For the present analysis a response spectrum in terms of accelerations *vs* period, *T* is assumed. This spectrum is computed from the *North-South component of El Centro earthquake* scaled by a factor of *2* and is shown in table 3.

Table 3 – The EL Centro's N-S component acceleration response spectrum scaled up by a factor of 2 for critical damping ratio, $\xi = 5\%$

a (m/s^2)	6.26	9.58	14.5	13.8	15.4	15.3	18.1	14.7	9.92	10.3	10.0
	0	0.01	0.11	0.21	0.31	0.41	0.51	0.61	0.71	0.81	0.91

It should be noticed that the response spectrum used is only considered for periods up to 0.91 sec. In fact, as shown in table A.2.1, the period of the first mode is 0.90 seconds making it pointless to compute the response analysis with spectrum values for periods greater than this as all the other modes will have lower periods.

Because the present analysis is merely an example, simplifications are assumed. For instance the response spectrum above is used regardless the soil nature. It is known that the soil characteristics influence a great deal the way the seismic waves reach a structure and affect its dynamical behaviour. A correct analysis would require the consideration of the response spectrum corresponding to the soil conditions of the area where the bridge is built. Usually the soils are classified for earthquake analysis according to their consistence as soft or hard and/or according to the soil being sandy or argillaceous.

Another factor the designer needs to take into account is the geographical localization of the structure. In fact, depending on many factors, there are regions with a seismic intensity higher than others. In most of the Seismic Codes, this fact is taken into account by scaling up or down the given response spectra by means of regional coefficients. For the present case, a correct analysis would require the use of a response spectrum typical for Taiwan instead of El Centro's N-S component. Still, given the exemplificative nature of this text, it is decided to use the set of four regional coefficients, Z, in the Code of Taiwan. The maximum value is 0.4 and the minimum is 0.22. The structure analysed will be in a region for which the regional coefficient, Z, is 0.34, i.e. the expected earthquake intensity is scaled down to 85% of the one expected in the most sensitive region.

For each direction, transverse, longitudinal and vertical, response spectrum loads are created from the response spectrum shown in table 3. It is not usual to use the same response spectrum to compute the vertical loading as done in this example. In fact the vertical motions are generally of a lower intensity than horizontal. For the present analysis, this is taken into account by reducing the vertical action using a coefficient, α_v, equal to 2/3.

Since the mode frequencies were very close, it is decided to adopt the CQC modal combination.

The behaviour coefficient assumed, η, is 2, i.e. internal forces evaluated by means of linear analysis are reduced to 50%.

It should be noted that since the earthquake action is in the form of an excitation, the analysis using response spectra provides an envelope of the response, Therefore the results are presented regardless of the sign. Thus the designer is requested a critical attitude when analysing the results attained.

Before discussing the results for the present bridge it is worth to make the following consideration with respect to the modal participation factors of the modes shown in the figures of Appendix A.2.

Table 4 – Modal Participation Factors for modes 1, 2 and 3.

	Transverse direction	Longitudinal direction	Vertical direction
Mode 1	0.01	*201.73*	0.94
Mode 2	*166.02*	0.22	5.46
Mode 3	2.84	5.87	*124.2*

As referred in the end of paragraph 2.11 the modal participation factor, P_{nJ}, is a good measure of the contribution of the *n*th mode for the global response in *J* direction. This may easily be confirmed by comparing the figures in the Appendix with the results in table 4. In fact it is observed that for each mode the largest modal participation factor is achieved precisely for the predominant direction of the displacements.

6.4 Results of the Response Spectrum Analysis

The results obtained are processed in a different manner according to the direction of the loading and its type (displacements or forces in the members). In the following these results are presented separately.

The results to be presented correspond to the members and joints identified in the figures in Appendix A.1.

Internal forces due to earthquake loading in horizontal direction

For this type of results, non-linear behaviour is allowed and therefore the reduction factor, η, is used as discussed in paragraph 4.3.

As is defined in some modern seismic codes for earthquake analysis, the *Design Specifications* elaborated by the *Taiwan High Speed Rail Corporation*, allow the designer to reduce the member forces considering to structural type of the system using a coefficient, α_y, equal to 1.25. The coefficient α_y may be defined as the ratio of the seismic design action used to the seismic design action leading to formation of a sufficient number of plastic hinges for overall structural instability.

Therefore the reduction coefficient adopted for multiplying the internal member forces due to earthquake loading in the horizontal direction is given by:

$$\frac{Z}{\alpha_y \cdot \eta} = \frac{0{,}34}{1{,}25 \times 2} = 0{,}136 \qquad (6.1)$$

Tables A.3.1 to A.3.4 in the Appendix A.3 present the reduced internal member forces for both earthquake loadings in transverse and longitudinal direction.

Internal forces due to earthquake loading in vertical direction

Usually ductility is not taken into account to compute the internal forces obtained when the earthquake acts under vertical direction. This is due to the fact that the response is mainly influenced by the vertical vibration modes, which are normally associated with brittle behaviour. So the reduction coefficient will be of the same form as in (6.1) assuming η equals to the unity.

$$\frac{\alpha_v \cdot Z}{\alpha_y} = \frac{2/3 \times 0{,}34}{1{,}25} = 0{,}181 \tag{6.2}$$

Tables A.3.5 and A.3.6 in Appendix A.3 present the reduced internal member forces for earthquake loading in vertical direction.

Displacements

The displacements were reduced by simply using the same coefficients for *Z* and α_v. Therefore the following reduction coefficients are considered:

- Displacements due to earthquake loading in horizontal direction:

$$Z = 0.34 \tag{6.3}$$

- Displacements due to earthquake loading in the vertical direction:

$$\alpha_v \cdot Z = 2/3 \cdot 0.34 = 0.227 \tag{6.4}$$

Tables A.3.7 to A.3.9 in Appendix A.3 present the reduced displacements.

Combination of Orthogonal Seismic Effects

To account for the directional uncertainty of earthquake motions and the simultaneous occurrences of the corresponding internal forces in three perpendicular directions, the results achieved are usually combined. For the present case the *Taiwan High Speed Rail Corporation* suggests the combination according to (6.5). The maximum displacement, internal force or moment, S_{max} is given by:

$$S_{\max} = \max \begin{Bmatrix} S_x + 0{,}3 \cdot S_y + 0{,}3 \cdot S_z \\ S_y + 0{,}3 \cdot S_x + 0{,}3 \cdot S_z \\ S_z + 0{,}3 \cdot S_x + 0{,}3 \cdot S_y \end{Bmatrix} \tag{6.5}$$

6.5 Time-History Response Analysis of the Bridge

Once the modal frequencies and the vibration mode shapes are computed, a time history analysis may be performed.

Considering the exemplificative nature of this analysis and, and the simplification used previously for the response spectra analysis, only the North – South component of the El Centro's accelerogram scaled up by a factor of 2 is used to compute the three earthquake loadings. Each load corresponds to the application of El Centro's N-S component in one direction of the bridge. Figure 17 represents the acceleration plot of the N-S component of the El Centro earthquake.

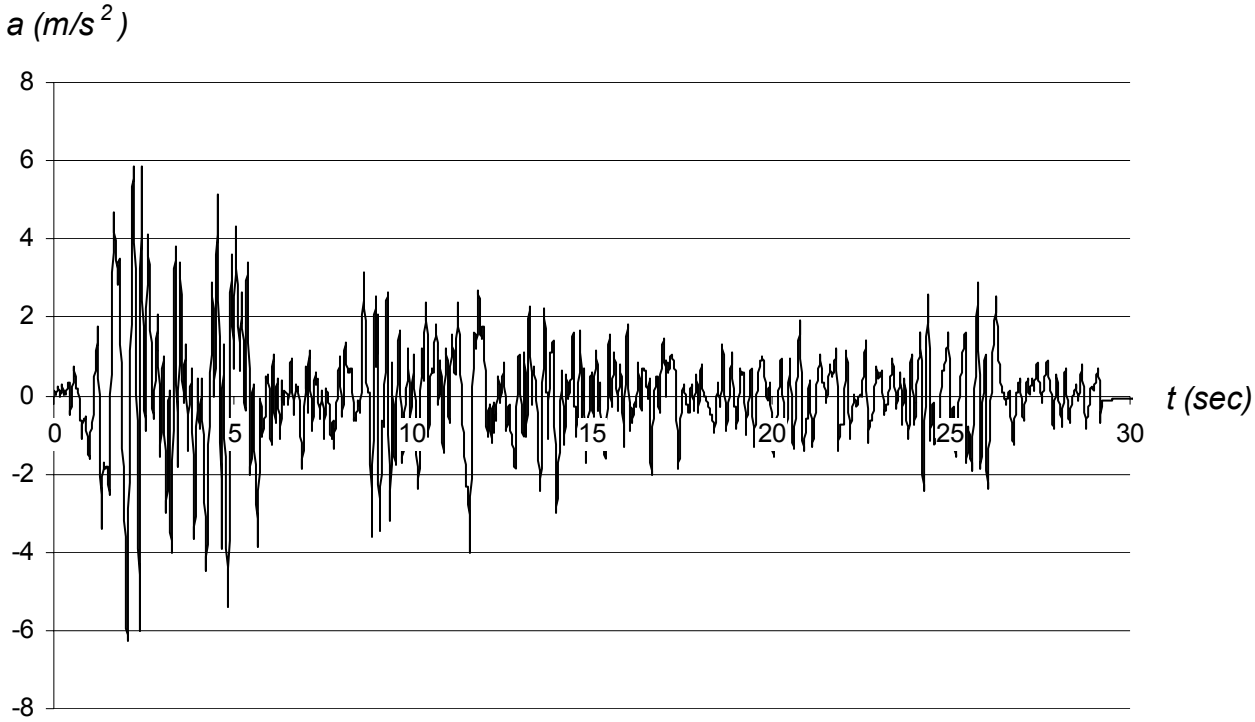

Figure 17 – Accelerogram of the N-S component of the El Centro earthquake scaled up by a factor of 2

A complete time history analysis of this bridge would require the use of three components of the acceleration vector. In this case two situations would have to be considered corresponding to the application of each horizontal acceleration component for both transverse and longitudinal direction of the bridge.

As in chapter 6.3 the considerations about the coefficients related to the soil nature, to the regional coefficients and to the vertical direction apply here.

6.6 Results of the Time-History Response Analysis

The results are computed in the same way as in the response spectrum analysis. This is due to the fact that both analyses rest on the mode superposition method based on the assumption that the system behaves linearly.

Therefore, in this analysis the same values for the reduction coefficients as adopted for the response spectrum analysis are used.

Tables A.4.1 to A.4.9 present the results similar to the ones presented in tables A.3.1 to A.3.9. Each result refers to the maximum value during the whole time history reduced by applying the reduction coefficients summarized here:

- Member forces due to horizontal earthquake loading: 0.136
- Member forces due to vertical earthquake loading: 0.181
- Displacements due to horizontal earthquake loading: 0.340
- Displacements due to vertical earthquake loading: 0.227

Because the same accelerogram is used to define the support acceleration in the three directions, *X*, *Y* and *Z*, to account for the directional uncertainty of the earthquake motions and the low probability of simultaneous occurrence of the maximum response for each direction, the rule presented in (6.5) may be applied again. It should be noted that the value *S* is to be inserted regardless of the sign.

As mentioned the time-history method allows a much more complete analysis because it provides the time evolution of any kind of result. The graphs shown in the following provide some examples of time variation of certain results.

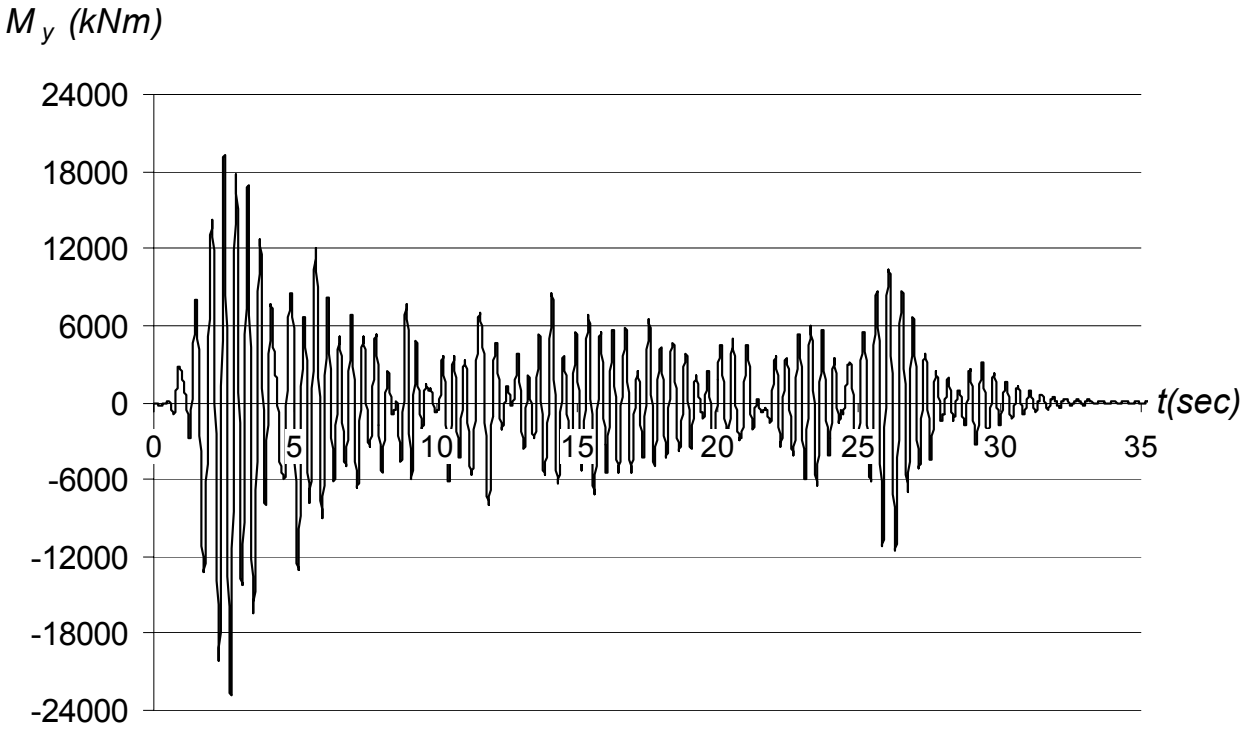

Figure 18 – Time variation of the moment at the base of pier 1 due to earthquake loading in the transverse direction

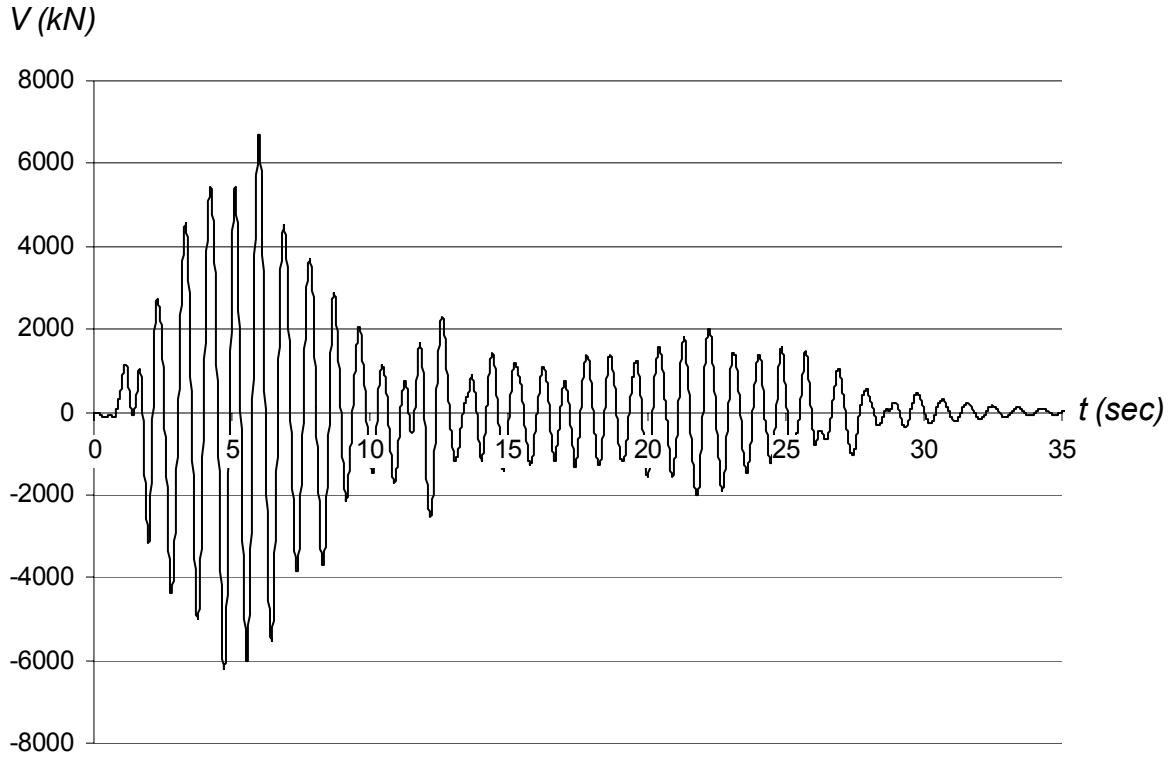

Figure 19 – Time variation of the shear force in longitudinal direction at base of pier 2 due to earthquake loading in the longitudinal direction

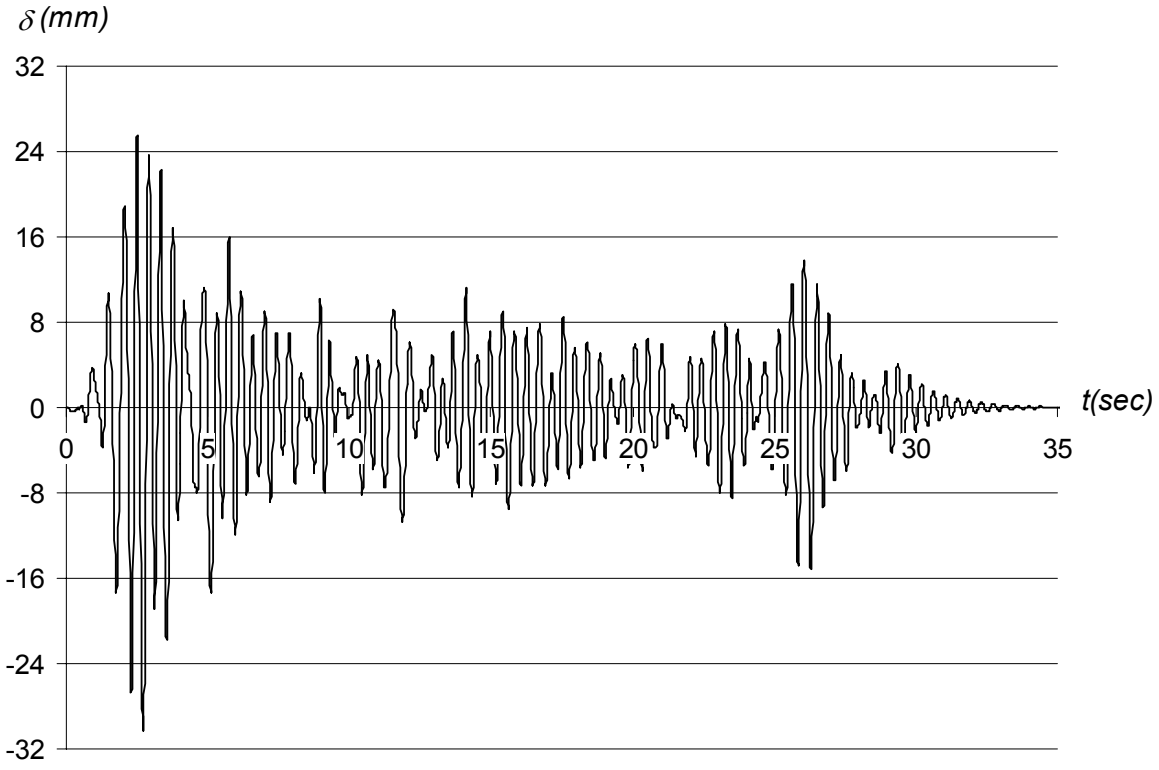

Figure 20 – Time variation of the transverse displacement at mid-span section of the middle span due to earthquake loading in the transverse direction

6.7 Equivalent Static Analysis of the Bridge

As discussed in chapter 5, this method provides good results when applied to structures meeting certain "regularity" conditions with respect to geometry, stiffness and mass distribution. Bridges are not usually part of this group of structures as they are normally rather complex. Moreover, bridges are often important infrastructures in social and economic terms, which implies a more careful analysis used in the design. Therefore equivalent static analysis is normally used only in the pre-design phase for this type of structures. However in this paragraph we illustrate the application of this method by computing the base shear force when the earthquake is in the transverse direction.

The *Design Specifications of the Taiwan High Speed Rail Corporation* prescribe that the bridge shall be designed and constructed to resist a minimum lateral seismic force, V, given by the expression:

$$V = \frac{Z}{\alpha_y \cdot \eta} \cdot S_a(T) \cdot \frac{W_{tot}}{g} \tag{6.6}$$

where

- T is the fundamental period in the direction under consideration. Since we use a simplified method, this parameter may be determined by the Rayleigh method which gives T=0.65 sec for the longitudinal direction (cf. paragraph 6.2);
- $S_a(T)$ is the acceleration corresponding to the fundamental period determined by means of a typical response spectrum. In this case, as in the previous analyses, we use the N-S component of the El Centro earthquake scaled up by a factor of 2. The value for the acceleration is computed from table 3 by linear interpolation and is equal to 12.6 m/s^2;
- W_{tot} is the total weight of the structure accounting for the train loads. $W_{tot} = 72\,894 kN$ and
- Z, α_y and η have the same meaning as in the previous analyses.

The base shear force for the earthquake acting in the transverse direction, V_z, is:

$$V_z = 0.136 \times 12.6 \times \frac{72\,894}{9.81} = 12\,734\ kN \tag{6.7}$$

As expected, this value is higher than the ones obtained using the previous analyses. For instance, consider the results from the response spectrum analysis for the shear force in the longitudinal direction in the support joints (2 and 5) when the earthquake acts in the same direction (see table A.3.4). The sum of these internal forces equals 10 019 kN. In fact, as discussed in paragraph 2.12, the deformed shape from the inertia loading is an approximation to the natural vibration shape and therefore introduces additional stiffness/frequency and consequently higher internal forces in the structure.

It should be noted that expression (6.7) is to be applied for each direction of the bridge so that a complete set of internal forces and displacements may be obtained. This implies the determination of the fundamental period for the three directions.

As in the previous analyses a combination rule such as in (6.5) should be applied to obtain the maximum design values in terms of displacements and internal forces.

References

[1] **R.W. Clough and Joseph Penzien**, Dynamics of Structures, McGraw-Hill, 1975

[2] **Mario Paz**, Structural Dynamics: Theory and Computation – third edition, Van Nostrand Reinhold, 1991.

[3] **CEN - European Committee for Standardization**, Eurocode 8: Design of structures for earthquake resistance - Part 1, Draft No 6, 2003.

[4] **Luís Guerreiro**, Revisões de análise modal e análise sísmica por espectros de resposta, Reprografia DECivil – Instituto Superior Técnico, 1999.

[5] **João Azevedo and Jorge Proença**, Dinâmica de estruturas, Reprografia DECivil – Instituto Superior Técnico, 1991.

[6] **Design Specifications**, Taiwan High Speed Rail Corporation, 2000.

Appendix

A.1 Model Identification

- Members Identification
- Joints Identification

Joints

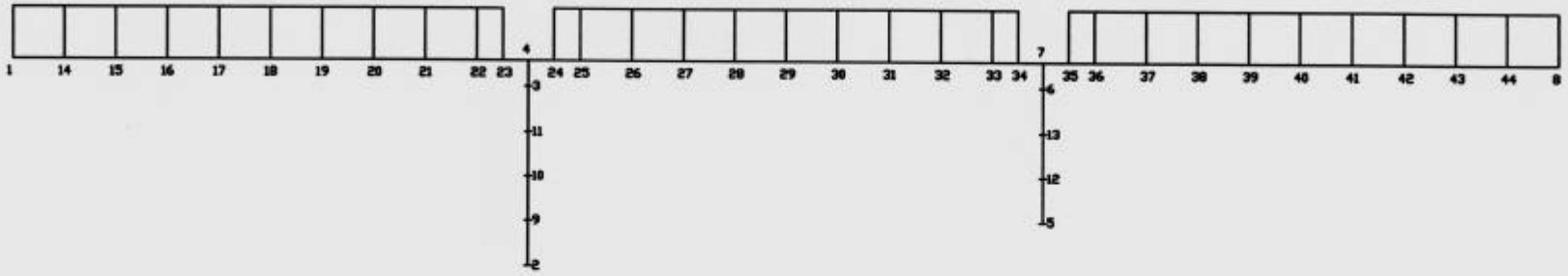

Members

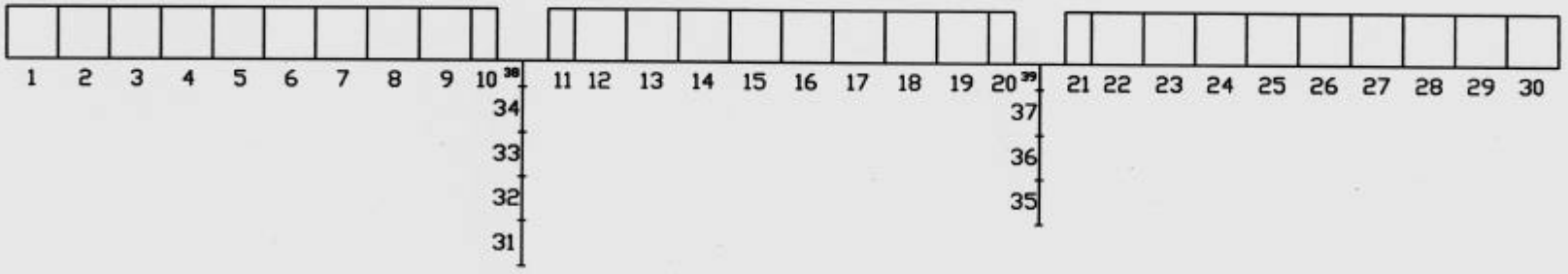

A.2 Eigen – Value Solution

- Table A.2.1
- Deformed Shapes
  i. Mode 1
  ii. Mode 2
  iii. Mode 3
  iv. Mode 1 applying the Rayleigh Method

Mode	Eigenvalue (rad/sec2)	Frequency (Hz)	Period (sec)	Mass participation (%)		
				X	Y	Z
1	4,83E+01	1,11	0,904	94,747	0,002	0,000
2	2,23E+02	2,37	0,421	0,000	0,072	66,490
3	5,65E+02	3,78	0,264	0,080	37,217	0,019
4	5,70E+02	3,80	0,263	0,514	10,163	0,005
5	6,68E+02	4,11	0,243	0,007	21,406	0,039
6	1,09E+03	5,26	0,190	0,000	0,002	0,087
7	3,42E+03	9,31	0,107	0,000	0,000	9,956
8	4,21E+03	10,32	0,097	0,001	0,022	0,005
9	5,44E+03	11,74	0,085	0,000	0,001	4,589
10	7,25E+03	13,55	0,074	0,876	0,039	0,078
11	7,45E+03	13,73	0,073	0,259	0,632	0,120
12	7,54E+03	13,82	0,072	0,083	0,000	0,132
13	8,02E+03	14,25	0,070	0,369	1,018	0,000
14	1,04E+04	16,26	0,061	0,000	0,002	0,003
15	1,15E+04	17,05	0,059	0,000	0,003	0,080
16	1,29E+04	18,06	0,055	0,061	0,343	0,001
17	1,32E+04	18,30	0,055	0,236	0,647	0,004
18	1,56E+04	19,86	0,050	0,119	1,224	0,041
19	1,63E+04	20,34	0,049	0,011	5,519	0,023
20	1,77E+04	21,19	0,047	0,067	2,082	0,013
21	1,81E+04	21,42	0,047	0,011	0,011	3,106
22	1,84E+04	21,59	0,046	0,106	0,100	0,061
23	1,93E+04	22,10	0,045	0,070	0,244	0,637
24	1,99E+04	22,48	0,044	0,122	1,384	0,492
25	2,01E+04	22,56	0,044	0,016	0,856	1,451
26	2,08E+04	22,94	0,044	0,054	3,189	0,033
27	2,25E+04	23,89	0,042	0,294	0,265	0,002
28	2,75E+04	26,38	0,038	0,516	0,059	0,016
29	2,92E+04	27,19	0,037	0,001	21,406	0,000
30	3,11E+04	28,05	0,036	0,008	0,036	0,136
31	3,30E+04	28,89	0,035	0,001	0,036	0,082
32	3,94E+04	31,57	0,032	0,000	0,016	0,389
33	4,81E+04	34,91	0,029	0,003	0,297	0,110
34	5,01E+04	35,62	0,028	0,053	0,068	0,070
35	5,49E+04	37,31	0,027	0,067	0,632	0,001
36	5,69E+04	37,97	0,026	0,000	0,064	0,616
37	6,48E+04	40,52	0,025	0,029	0,012	0,408
38	6,59E+04	40,85	0,024	0,000	0,032	0,003
39	6,89E+04	41,79	0,024	0,001	0,000	0,667
40	7,66E+04	44,04	0,023	0,012	0,000	0,890
41	7,72E+04	44,22	0,023	0,014	0,647	0,130
42	8,72E+04	47,01	0,021	0,355	0,007	0,183
43	9,01E+04	47,77	0,021	0,027	0,006	0,386
44	9,91E+04	50,11	0,020	0,020	0,027	0,961
45	1,06E+05	51,72	0,019	0,005	0,024	0,022
46	1,09E+05	52,61	0,019	0,001	0,000	0,004
47	1,10E+05	52,77	0,019	0,016	0,244	0,053
48	1,25E+05	56,34	0,018	0,015	0,003	0,001
49	1,29E+05	57,18	0,017	0,000	0,077	0,116
50	1,34E+05	58,30	0,017	0,045	0,095	0,001
51	1,37E+05	58,95	0,017	0,087	0,099	0,061
Mode	Eigenvalue	Frequency	Period	Mass participation (%)		

Mode	Eigenvalue (rad/sec2)	Frequency (Hz)	Period (sec)	Mass participation (%) X	Y	Z
52	1,53E+05	62,15	0,016	0,003	0,109	0,064
53	1,55E+05	62,69	0,016	0,032	0,059	0,017
54	1,60E+05	63,73	0,016	0,007	0,132	0,000
55	1,74E+05	66,43	0,015	0,035	0,009	0,015
56	1,77E+05	66,99	0,015	0,024	0,027	0,047
57	1,86E+05	68,57	0,015	0,001	0,018	0,003
58	1,90E+05	69,46	0,014	0,026	0,039	0,008
59	1,95E+05	70,34	0,014	0,083	0,068	0,015
60	1,98E+05	70,78	0,014	0,049	0,007	0,051
61	2,12E+05	73,31	0,014	0,001	0,005	0,351
62	2,19E+05	74,56	0,013	0,001	0,000	0,004
63	2,27E+05	75,81	0,013	0,001	0,004	0,000
64	2,28E+05	76,00	0,013	0,004	0,008	0,145
65	2,32E+05	76,70	0,013	0,006	0,000	0,136
66	2,37E+05	77,41	0,013	0,002	0,002	0,747
67	2,47E+05	79,05	0,013	0,026	0,002	0,011
68	2,61E+05	81,36	0,012	0,000	0,006	0,002
69	2,72E+05	82,99	0,012	0,002	0,000	0,169
70	2,90E+05	85,71	0,012	0,037	0,030	0,043
71	2,99E+05	87,06	0,011	0,087	0,000	0,097
72	3,06E+05	88,03	0,011	0,002	0,017	0,216
73	3,10E+05	88,66	0,011	0,002	0,004	0,183
74	3,13E+05	89,03	0,011	0,000	0,022	0,105
75	3,20E+05	90,02	0,011	0,015	0,379	0,143
76	3,26E+05	90,90	0,011	0,007	0,536	0,072
77	3,45E+05	93,47	0,011	0,024	0,109	0,000
78	3,61E+05	95,62	0,010	0,000	0,002	0,004
79	3,66E+05	96,26	0,010	0,000	0,004	0,036
80	3,80E+05	98,10	0,010	0,007	0,044	0,000
81	3,87E+05	99,03	0,010	0,053	0,003	0,000
82	4,20E+05	103,13	0,010	0,000	0,032	0,015
83	4,34E+05	104,79	0,010	0,012	0,039	0,001
84	4,74E+05	109,53	0,009	0,000	0,004	0,000
85	4,87E+05	111,09	0,009	0,000	0,000	0,119
86	4,94E+05	111,83	0,009	0,000	0,193	0,029
87	5,20E+05	114,80	0,009	0,008	0,405	0,174
88	5,37E+05	116,59	0,009	0,017	0,018	0,034
89	5,39E+05	116,85	0,009	0,019	0,008	0,072
90	5,60E+05	119,14	0,008	0,009	0,001	0,179
91	5,68E+05	119,94	0,008	0,000	0,028	0,000
92	5,74E+05	120,55	0,008	0,007	0,027	0,011
93	5,79E+05	121,16	0,008	0,018	0,019	0,000
94	5,92E+05	122,43	0,008	0,001	0,025	0,178
95	5,97E+05	123,02	0,008	0,001	0,030	0,402
96	6,15E+05	124,79	0,008	0,000	0,000	0,002
97	6,27E+05	126,06	0,008	0,000	0,000	0,018
98	6,59E+05	129,24	0,008	0,000	0,001	0,003
99	6,85E+05	131,68	0,008	0,000	0,152	0,000
100	7,07E+05	133,81	0,007	0,000	0,060	0,003
101	7,10E+05	134,13	0,007	0,000	0,536	0,000
102	7,28E+05	135,78	0,007	0,000	0,000	0,041

103	7,58E+05	138,57	0,007	0,000	0,003	0,000
104	7,68E+05	139,52	0,007	0,000	0,000	0,002
105	8,12E+05	143,41	0,007	0,000	0,001	0,031
106	8,23E+05	144,41	0,007	0,000	0,000	0,065
107	8,29E+05	144,88	0,007	0,000	0,032	0,021
108	9,08E+05	151,66	0,007	0,000	0,011	0,000
109	9,65E+05	156,33	0,006	0,000	0,003	0,010
110	9,83E+05	157,79	0,006	0,000	0,022	0,306
111	9,97E+05	158,96	0,006	0,000	0,074	0,038
112	1,05E+06	163,00	0,006	0,000	0,000	0,005
113	1,07E+06	164,30	0,006	0,000	0,018	0,000
114	1,08E+06	165,74	0,006	0,000	0,017	0,018
115	1,09E+06	166,30	0,006	0,000	0,046	0,017
116	1,12E+06	168,73	0,006	0,000	0,000	0,002
117	1,15E+06	170,54	0,006	0,000	0,000	0,000
118	1,15E+06	170,61	0,006	0,000	0,002	0,021
119	1,17E+06	171,89	0,006	0,000	0,025	0,000
120	1,22E+06	176,01	0,006	0,000	0,000	0,000
121	1,29E+06	181,10	0,006	0,000	0,000	0,002
122	1,33E+06	183,64	0,005	0,000	0,039	0,036
123	1,42E+06	189,47	0,005	0,000	0,020	0,031
124	1,44E+06	190,78	0,005	0,000	0,002	0,079
125	1,45E+06	191,76	0,005	0,000	0,060	0,438

Deformed Shape – Mode 1

i. Isometric view
ii. X-Y Plane view

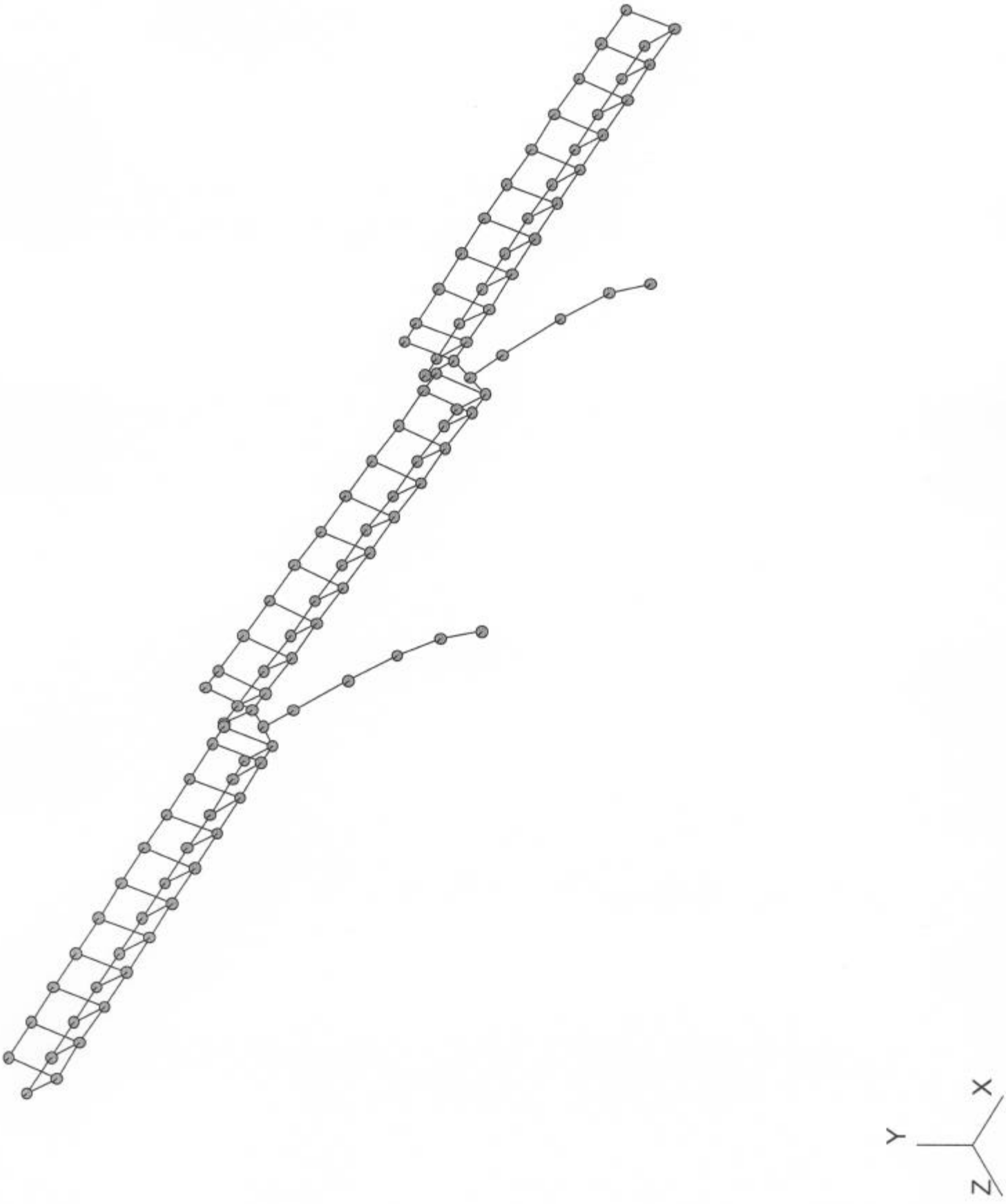
X
Y
Z

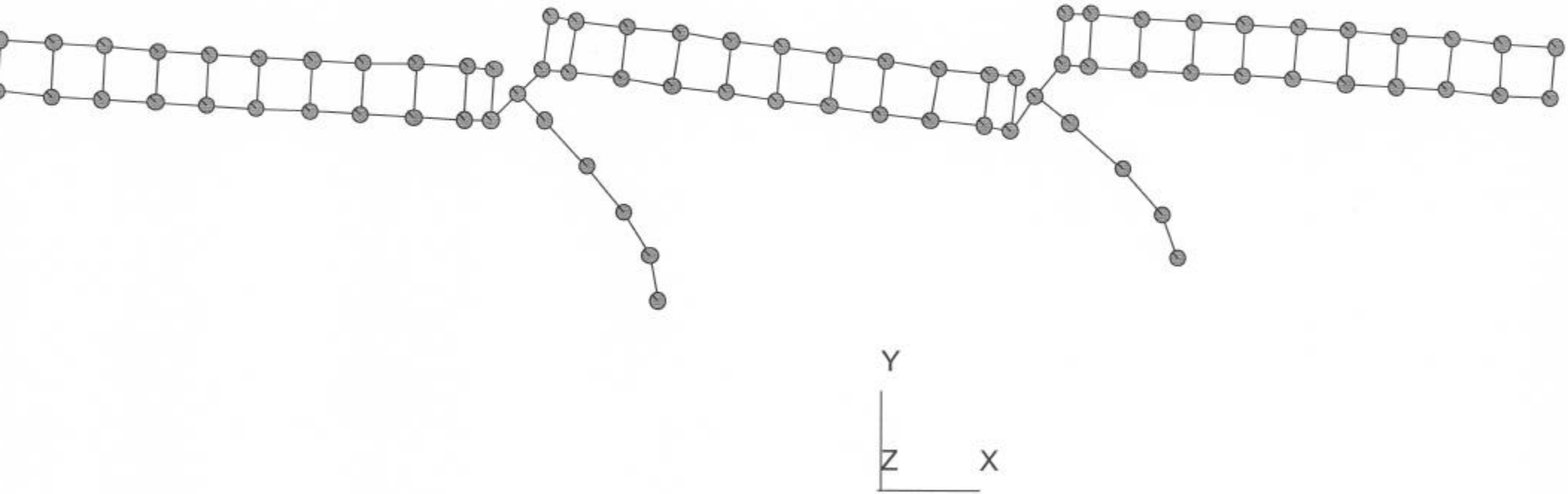
Y
Z
X

Deformed Shape – Mode 2

i. Isometric view
ii. X-Z Plane view

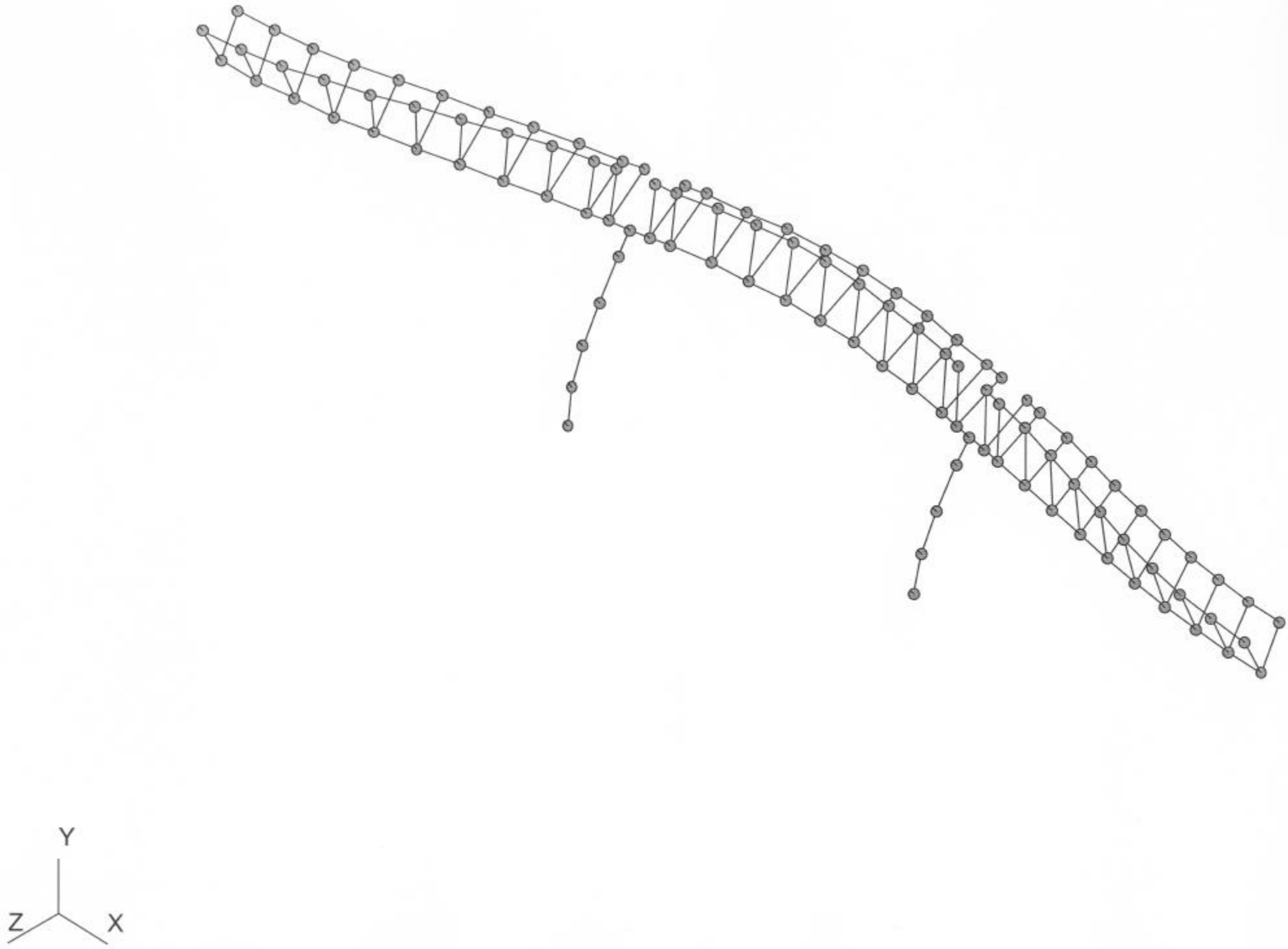
Y
Z
X

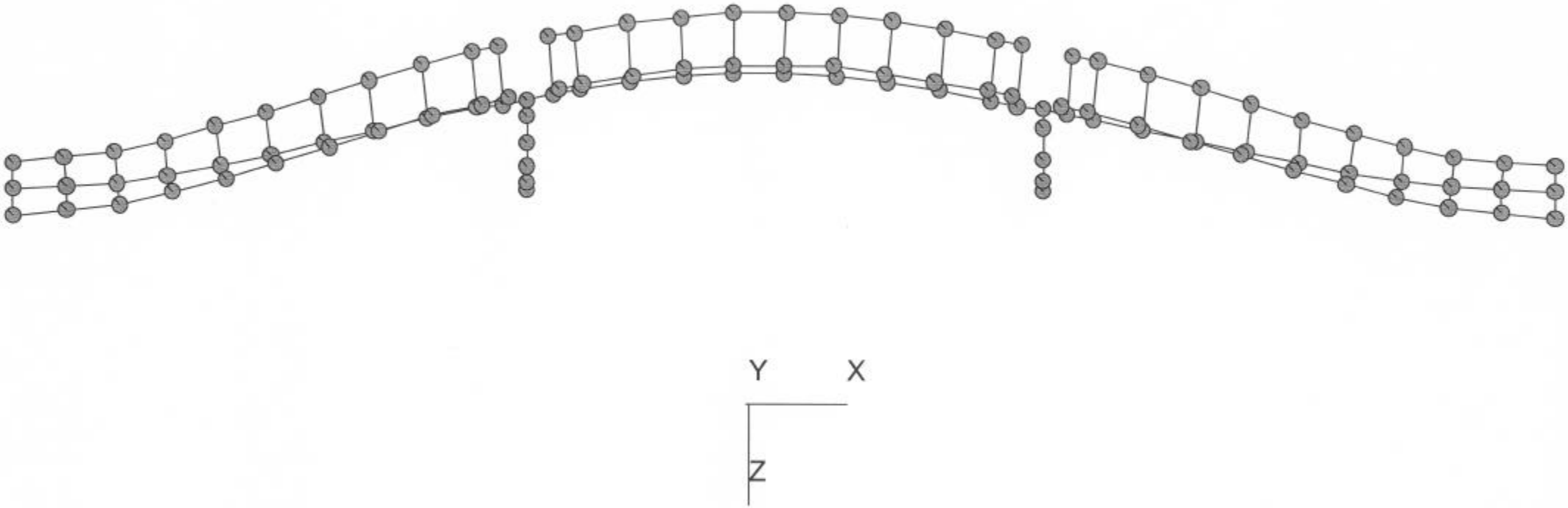
Y
X
Z

Deformed Shape – Mode 3

i. Isometric view
ii. X-Y Plane view

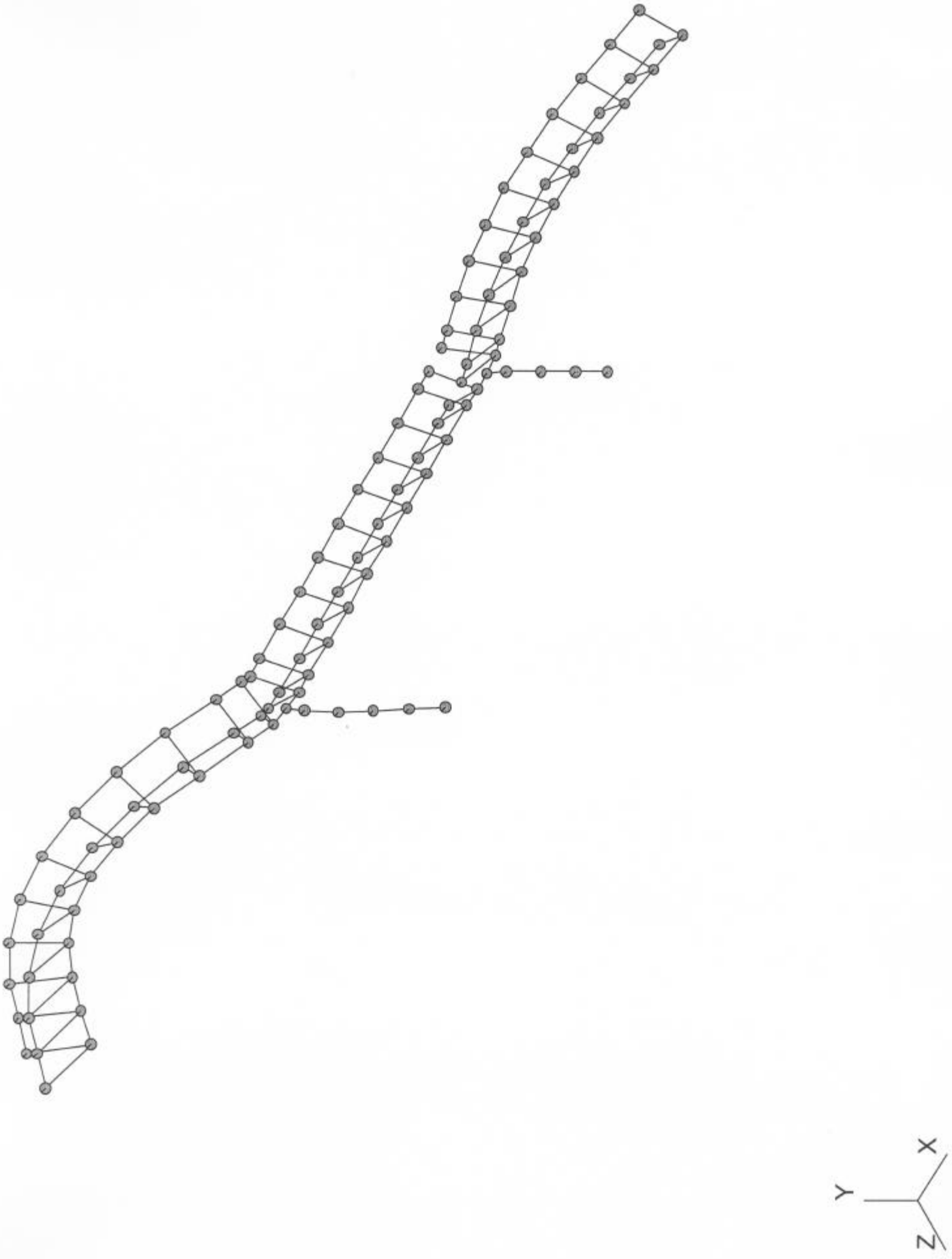
X
Y
Z

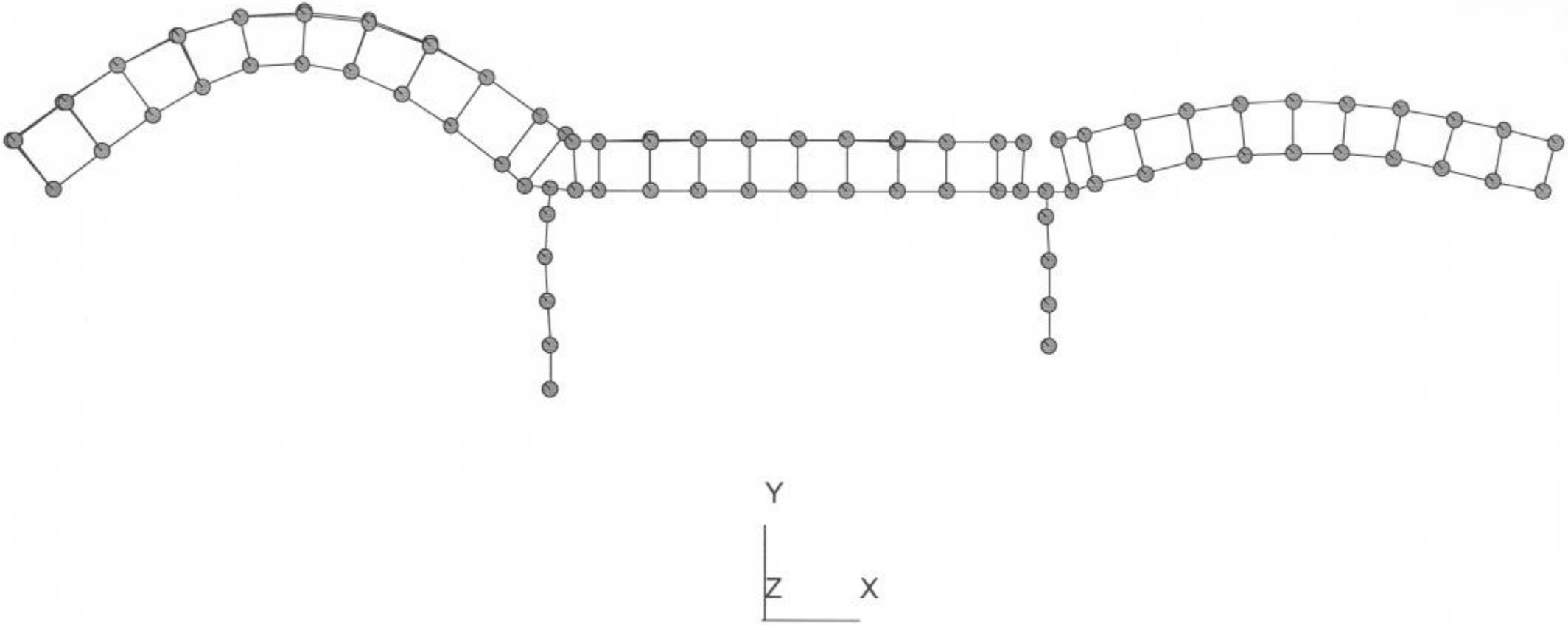
Y
Z
X

Deformed Shape – Mode 1 – using the Rayleigh method

---

i. Isometric view
ii. X-Y Plane view

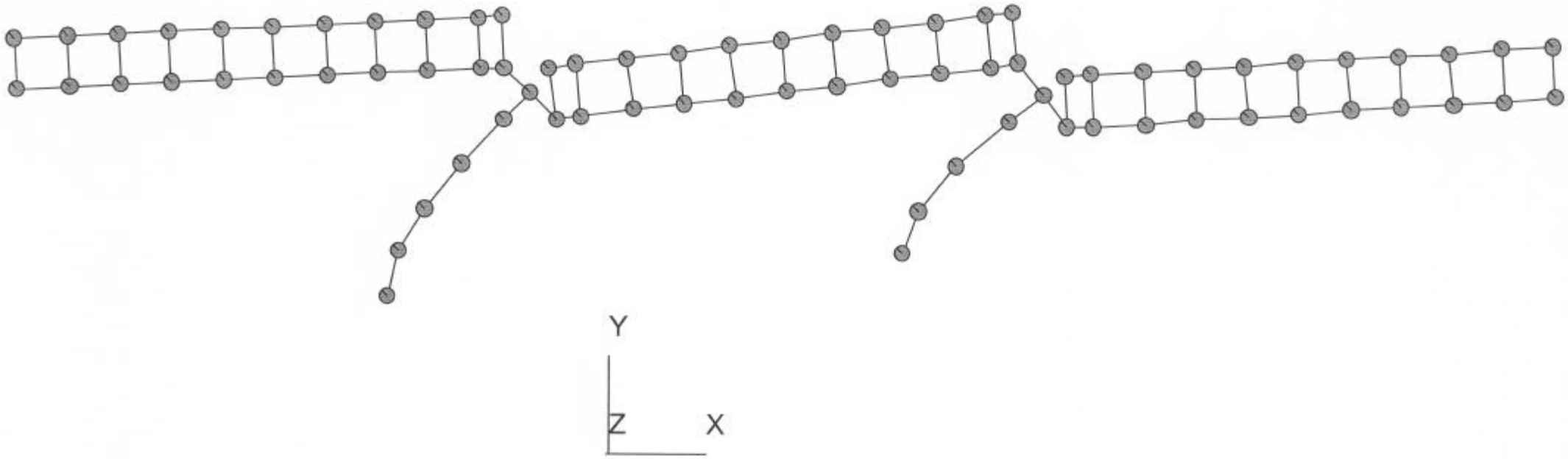
Y
Z
X

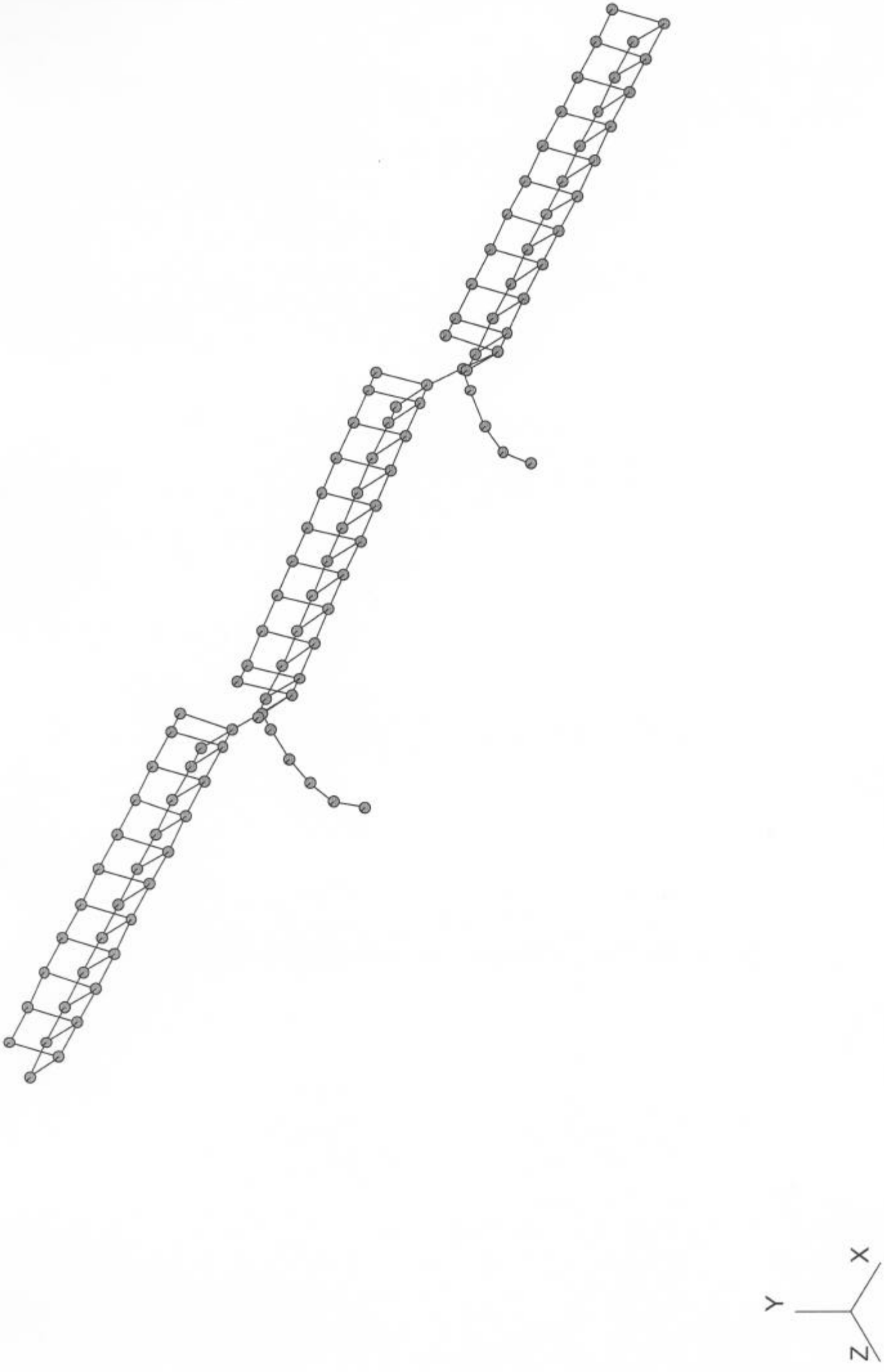
X
Y
Z

A.3 Tables of Results for Response Spectra Analysis

---

i. Internal Forces in the Girder – Transverse Loading
ii. Internal Forces in the Piers – Transverse Loading
iii. Internal Forces in the Girder – Longitudinal Loading
iv. Internal Forces in the Piers – Longitudinal Loading
v. Internal Forces in the Girder – Vertical Loading
vi. Internal Forces in the Piers – Vertical Loading
vii. Displacements – Transverse Loading
viii. Displacements – Longitudinal Loading
ix. Displacements – Vertical Loading

Table A.3.1 - Member Forces in the Girder - Earthquake loading in transverse direction (kN-m)

			Forces				Moments	
Span ID	**Element**	**Joint**	**Axial**	**Shear Y**	**Shear Z**	**Torsion**	**Bending Y**	**Bending Z**
1	1	**1**	**0**	**57**	***3230***	**8454**	***74744***	**0**
		14	10	57	*3230*	8454	*61962*	227
	2	14	10	57	*3230*	8454	*61962*	227
		15	17	47	*3203*	8397	*49224*	442
	3	15	17	47	*3203*	8397	*49224*	442
		16	20	40	*3081*	7978	*36822*	583
	4	16	20	40	*3081*	7978	*36822*	583
		17	22	32	*2994*	7878	*24838*	672
	5	17	22	32	*2994*	7878	*24838*	672
		18	**27**	**21**	***2840***	**7657**	***13773***	**691**
	6	18	27	21	*2840*	7657	*13773*	691
		19	32	21	*2632*	7369	*5594*	634
	7	19	32	21	*2632*	7369	*5594*	634
		20	35	32	*2404*	7139	*9307*	527
	8	20	35	32	*2404*	7139	*9307*	527
		21	39	42	*2132*	6867	*17166*	366
	9	21	39	42	*2132*	6867	*17166*	366
		22	42	56	*1787*	6742	*24033*	142
	10	22	42	56	*1787*	6742	*24033*	142
		23	**44**	**63**	***1513***	**6469**	***26992***	**0**
2	11	**24**	**47**	**96**	***2052***	**3413**	***31121***	**0**
		25	47	96	*2052*	3413	*35119*	194
	12	25	47	96	*2052*	3413	*35119*	194
		26	51	87	*1529*	3115	*40991*	535
	13	26	51	87	*1529*	3115	*40991*	535
		27	55	68	*914*	2520	*44393*	790
	14	27	55	68	*914*	2520	*44393*	790
		28	56	47	*419*	2027	*45763*	963
	15	28	56	47	*419*	2027	*45763*	963
		29	**58**	**25**	***284***	**1524**	***44940***	**1039**
	16	29	58	25	*284*	1524	*44940*	1039
		30	57	20	*848*	850	*41618*	982
	17	30	57	20	*848*	850	*41618*	982
		31	55	51	*1453*	762	*35850*	801
	18	31	55	51	*1453*	762	*35850*	801
		32	52	70	*1965*	1061	*28047*	536
	19	32	52	70	*1965*	1061	*28047*	536
		33	49	91	*2552*	1470	*17987*	191
	20	33	49	91	*2552*	1470	*17987*	191
		34	**46**	**98**	***2872***	**1713**	***12311***	**0**
3	21	**35**	**44**	**65**	***715***	**7657**	***9704***	**0**
		36	44	65	*715*	7657	*8884*	132
	22	36	44	65	*715*	7657	*8884*	132
		37	41	57	*1023*	7945	*6284*	374
	23	37	41	57	*1023*	7945	*6284*	374
		38	38	43	*1292*	8044	*5421*	542
	24	38	38	43	*1292*	8044	*5421*	542
		39	35	31	*1521*	8313	*9275*	655
	25	39	35	31	*1521*	8313	*9275*	655
		40	**31**	**17**	***1719***	**8539**	***15527***	**705**
	26	40	31	17	*1719*	8539	*15527*	705
		41	27	16	*1908*	8809	*22930*	680
	27	41	27	16	*1908*	8809	*22930*	680
		42	23	30	*2053*	9012	*31072*	582
	28	42	23	30	*2053*	9012	*31072*	582
		43	20	41	*2137*	9103	*39659*	431
	29	43	20	41	*2137*	9103	*39659*	431
		44	15	51	*2243*	9448	*48680*	236
	30	44	15	51	*2243*	9448	*48680*	236
		8	**0**	**59**	***2265***	**9476**	***57721***	**0**

Table A.3.2 - Member forces in the Piers - Earthquake loading in transverse direction (kN-m)

			Forces				Moments	
Pier ID	**Element**	**Joint**	**Axial**	**Shear Y**	**Shear Z**	**Torsion**	**Bending Y**	**Bending Z**
1	31	**2**	**172**	**19**	***1737***	**2876**	***22935***	**77**
		9	172	19	*1737*	2876	*16897*	20
	32	9	172	19	*1737*	2876	*16897*	20
		10	172	15	*1717*	2874	*11125*	38
	33	10	172	15	*1717*	2874	*11125*	38
		11	171	14	*1658*	2871	*5630*	76
	34	11	171	14	*1658*	2871	*5630*	76
		3	169	15	*1547*	2865	*1583*	118
	38	3	169	15	*1547*	2865	*1583*	118
		4	**167**	**15**	***1338***	**2848**	***3085***	**142**
2	35	**5**	**174**	**19**	***3242***	**4065**	***33124***	**65**
		12	174	19	*3242*	4065	*21957*	11
	36	12	174	19	*3242*	4065	*21957*	11
		13	174	16	*3218*	4062	*11058*	53
	37	13	174	16	*3218*	4062	*11058*	53
		6	173	16	*3143*	4057	*1276*	103
	39	6	173	16	*3143*	4057	*1276*	103
		7	**171**	**16**	***2967***	**4039**	***6077***	**133**

Table A.3.3 - Member Forces in the Girder - Earthquake loading in longitudinal direction (kN-m)

Span ID	Element	Joint	Forces				Moments	
			Axial	Shear Y	Shear Z	Torsion	Bending Y	Bending Z
1	1	**1**	***0***	**249**	**24**	**100**	**145**	**0**
		14	*254*	249	24	100	117	997
	2	14	*254*	249	24	100	117	997
		15	*669*	217	23	93	89	1780
	3	15	*669*	217	23	93	89	1780
		16	*1011*	171	21	75	88	2334
	4	16	*1011*	171	21	75	88	2334
		17	*1283*	132	21	58	93	2695
	5	17	*1283*	132	21	58	93	2695
		18	***1582***	**99**	**20**	**32**	**58**	**2751**
	6	18	*1582*	99	20	32	58	2751
		19	*1881*	92	20	28	55	2546
	7	19	*1881*	92	20	28	55	2546
		20	*2152*	114	20	37	68	2157
	8	20	*2152*	114	20	37	68	2157
		21	*2422*	156	20	49	82	1533
	9	21	*2422*	156	20	49	82	1533
		22	*2760*	215	20	64	97	643
	10	22	*2760*	215	20	64	97	643
		23	***2994***	**254**	**20**	**70**	**105**	**0**
2	11	**24**	***408***	**162**	**21**	**42**	**126**	**0**
		25	*408*	162	21	42	111	329
	12	25	*408*	162	21	42	111	329
		26	*754*	92	21	38	99	678
	13	26	*754*	92	21	38	99	678
		27	*1090*	73	22	34	84	663
	14	27	*1090*	73	22	34	84	663
		28	*1359*	112	22	42	77	498
	15	28	*1359*	112	22	42	77	498
		29	***1628***	**139**	**22**	**49**	**83**	**567**
	16	29	*1628*	139	22	49	83	567
		30	*1924*	126	22	43	63	809
	17	30	*1924*	126	22	43	63	809
		31	*2218*	80	22	30	73	929
	18	31	*2218*	80	22	30	73	929
		32	*2487*	49	22	35	97	849
	19	32	*2487*	49	22	35	97	849
		33	*2823*	97	21	53	112	432
	20	33	*2823*	97	21	53	112	432
		34	***3055***	**143**	**21**	**60**	**117**	**0**
3	21	**35**	***2972***	**328**	**20**	**94**	**103**	**0**
		36	*2972*	328	20	94	103	665
	22	36	*2972*	328	20	94	103	665
		37	*2625*	263	20	86	109	1816
	23	37	*2625*	263	20	86	109	1816
		38	*2290*	192	20	63	101	2582
	24	38	*2290*	192	20	63	101	2582
		39	*2022*	135	20	42	96	3074
	25	39	*2022*	135	20	42	96	3074
		40	***1753***	**96**	**21**	**29**	**98**	**3266**
	26	40	*1753*	96	21	29	98	3266
		41	*1457*	105	21	40	63	3175
	27	41	*1457*	105	21	40	63	3175
		42	*1160*	153	21	68	49	2766
	28	42	*1160*	153	21	68	49	2766
		43	*889*	205	21	84	57	2057
	29	43	*889*	205	21	84	57	2057
		44	*551*	261	23	100	87	1115
	30	44	*551*	261	23	100	87	1115
		8	***0***	**297**	**23**	**110**	**133**	**0**

Table A.3.4 - Member forces in the Piers - Earthquake loading in longitudinal direction (kN-m)

Pier ID	Element	Joint	Forces				Moments	
			Axial	Shear Y	Shear Z	Torsion	Bending Y	Bending Z
1	31	**2**	**278**	***3319***	**9**	**2**	**36**	***51776***
		9	278	*3319*	9	2	12	*40166*
	32	9	278	*3319*	9	2	12	*40166*
		10	276	*3309*	7	2	22	*28925*
	33	10	276	*3309*	7	2	22	*28925*
		11	273	*3274*	5	2	37	*17804*
	34	11	273	*3274*	5	2	37	*17804*
		3	269	*3206*	5	2	48	*6614*
	38	3	269	*3206*	5	2	48	*6614*
		4	**263**	***3069***	**6**	**2**	**54**	***856***
2	35	**5**	**297**	***6700***	**12**	**3**	**47**	***82745***
		12	297	*6700*	12	3	16	*59634*
	36	12	297	*6700*	12	3	16	*59634*
		13	296	*6684*	11	3	40	*36911*
	37	13	296	*6684*	11	3	40	*36911*
		6	293	*6633*	9	3	69	*13710*
	39	6	293	*6633*	9	3	69	*13710*
		7	**287**	***6506***	**8**	**3**	**83**	***992***

Table A.3.5 - Member Forces in the Girder - Earthquake loading in vertical direction (kN-m)

			Forces				Moments	
Span ID	Element	Joint	Axial	Shear Y	Shear Z	Torsion	Bending Y	Bending Z
1	1	**1**	**0**	***2598***	**159**	**945**	**3583**	***0***
		14	31	*2598*	159	945	2964	*10394*
	2	14	31	*2598*	159	945	2964	*10394*
		15	79	*2240*	157	877	2335	*19428*
	3	15	79	*2240*	157	877	2335	*19428*
		16	115	*1671*	151	732	1723	*25828*
	4	16	115	*1671*	151	732	1723	*25828*
		17	142	*1046*	145	591	1142	*29903*
	5	17	142	*1046*	145	591	1142	*29903*
		18	**171**	***297***	**138**	**373**	**604**	***30744***
	6	18	171	*297*	138	373	604	*30744*
		19	193	*669*	128	400	232	*28168*
	7	19	193	*669*	128	400	232	*28168*
		20	199	*1373*	116	515	476	*22732*
	8	20	199	*1373*	116	515	476	*22732*
		21	196	*1960*	100	628	848	*14952*
	9	21	196	*1960*	100	628	848	*14952*
		22	182	*2452*	80	725	1145	*5341*
	10	22	182	*2452*	80	725	1145	*5341*
		23	**152**	***2592***	**67**	**735**	**1264**	***0***
2	11	**24**	**476**	***2169***	**119**	**601**	**1458**	***0***
		25	476	*2169*	119	601	1667	*4392*
	12	25	476	*2169*	119	601	1667	*4392*
		26	490	*1973*	87	589	1980	*12353*
	13	26	490	*1973*	87	589	1980	*12353*
		27	492	*1538*	55	495	2167	*18336*
	14	27	492	*1538*	55	495	2167	*18336*
		28	497	*1020*	30	368	2235	*22364*
	15	28	497	*1020*	30	368	2235	*22364*
		29	**501**	***401***	**29**	**211**	**2176**	***23880***
	16	29	501	*401*	29	211	2176	*23880*
		30	505	*384*	60	149	1974	*22472*
	17	30	505	*384*	60	149	1974	*22472*
		31	506	*1052*	95	406	1644	*18305*
	18	31	506	*1052*	95	406	1644	*18305*
		32	507	*1556*	123	527	1253	*12140*
	19	32	507	*1556*	123	527	1253	*12140*
		33	512	*1985*	151	622	887	*4351*
	20	33	512	*1985*	151	622	887	*4351*
		34	**508**	***2111***	**168**	**639**	**816**	***0***
3	21	**35**	**148**	***2648***	**46**	**787**	**821**	***0***
		36	148	*2648*	46	787	743	*5362*
	22	36	148	*2648*	46	787	743	*5362*
		37	162	*2446*	55	778	560	*15222*
	23	37	162	*2446*	55	778	560	*15222*
		38	168	*1962*	68	679	415	*22858*
	24	38	168	*1962*	68	679	415	*22858*
		39	171	*1377*	77	564	496	*28298*
	25	39	171	*1377*	77	564	496	*28298*
		40	**165**	***668***	**81**	**450**	**750**	***30866***
	26	40	165	*668*	81	450	750	*30866*
		41	146	*281*	85	414	1060	*30035*
	27	41	146	*281*	85	414	1060	*30035*
		42	118	*1046*	91	610	1400	*25898*
	28	42	118	*1046*	91	610	1400	*25898*
		43	92	*1676*	99	743	1767	*19249*
	29	43	92	*1676*	99	743	1767	*19249*
		44	65	*2250*	109	873	2169	*10489*
	30	44	65	*2250*	109	873	2169	*10489*
		8	**0**	***2610***	**114**	**932**	**2590**	***0***

Table A.3.6 - Member forces in the Piers - Earthquake loading in vertical direction (kN-m)

Pier ID	Element	Joint	Forces				Moments	
			Axial	Shear Y	Shear Z	Torsion	Bending Y	Bending Z
1	31	**2**	***4507***	**424**	**156**	**133**	**1333**	**1997**
		9	*4507*	424	156	133	842	554
	32	9	*4507*	424	156	133	842	554
		10	*4495*	414	153	133	492	935
	33	10	*4495*	414	153	133	492	935
		11	*4472*	398	147	132	548	2261
	34	11	*4472*	398	147	132	548	2261
		3	*4439*	385	138	132	910	3584
	38	3	*4439*	385	138	132	910	3584
		4	***4388***	**382**	**124**	**131**	**1133**	**4332**
2	35	**5**	***4446***	**522**	**224**	**192**	**1676**	**1938**
		12	*4446*	522	224	192	993	380
	36	12	*4446*	522	224	192	993	380
		13	*4434*	511	221	192	591	1672
	37	13	*4434*	511	221	192	591	1672
		6	*4412*	493	215	192	917	3369
	39	6	*4412*	493	215	192	917	3369
		7	***4373***	**484**	**205**	**191**	**1260**	**4322**

Table A.3.7 - Displacements - Earthquake loading in transverse direction

Joint	Translations (mm)			Rotations (rad)		
	X	Y	Z	X	Y	Z
1	0,0	0,0	***0,0***	0,0	0,0	0,0
8	0,0	0,0	***0,0***	0,0	0,0	0,0
18	0,0	0,4	***9,2***	0,1	0,0	0,0
4	0,0	0,0	***23,8***	0,1	0,0	0,0
29	0,0	0,6	***30,4***	0,1	0,0	0,0
7	0,0	0,0	***21,2***	0,1	0,0	0,0
40	0,0	0,4	***7,5***	0,1	0,0	0,0

Table A.3.8 - Displacements - Earthquake loading in longitudinal direction

Joint	Translations (mm)			Rotations (rad)		
	X	Y	Z	X	Y	Z
1	***73,5***	0,0	0,0	0,0	0,0	0,0
8	***73,0***	0,0	0,0	0,0	0,0	0,0
18	***73,3***	7,8	0,0	0,0	0,0	0,0
4	***73,0***	0,1	0,0	0,0	0,0	0,4
29	***72,9***	1,8	0,0	0,0	0,0	0,0
7	***72,5***	0,0	0,0	0,0	0,0	0,5
40	***72,8***	9,8	0,0	0,0	0,0	0,0

Table A.3.9 - Displacements - Earthquake loading in vertical direction

Joint	Translations (mm)			Rotations (rad)		
	X	Y	Z	X	Y	Z
1	0,2	***0,0***	0,0	0,0	0,0	0,0
8	0,2	***0,0***	0,0	0,0	0,0	0,0
18	0,2	***6,0***	0,1	0,0	0,0	0,0
4	0,2	***0,3***	0,4	0,0	0,0	0,2
29	0,2	***4,3***	0,5	0,0	0,0	0,0
7	0,2	***0,2***	0,3	0,0	0,0	0,2
40	0,2	***6,0***	0,1	0,0	0,0	0,0

A.4 Tables of Results for Time-History Analysis

---

i. Internal Forces in the Girder – Transverse Loading
ii. Internal Forces in the Piers – Transverse Loading
iii. Internal Forces in the Girder – Longitudinal Loading
iv. Internal Forces in the Piers – Longitudinal Loading
v. Internal Forces in the Girder – Vertical Loading
vi. Internal Forces in the Piers – Vertical Loading
vii. Displacements – Transverse Loading
viii. Displacements – Longitudinal Loading
ix. Displacements – Vertical Loading

Table A.4.1 - Member Forces in the Girder - Earthquake loading in transverse direction (kN-m)

			Forces				Moments	
Span ID	Element	Joint	Axial	Shear Y	Shear Z	Torsion	Bending Y	Bending Z
1	1	**1**	**0**	**66**	***3349***	**8163**	***-74498***	**0**
		14	8	-66	*-3349*	-8163	*61289*	264
	2	14	8	-66	*-3349*	-8163	*61289*	264
		15	-8	-57	*-3278*	-8074	*48635*	541
	3	15	-8	-57	*-3278*	-8074	*48635*	541
		16	7	-47	*-3095*	-7660	*36368*	718
	4	16	7	-47	*-3095*	-7660	*36368*	718
		17	-10	-34	*-2971*	-7557	*24420*	819
	5	17	-10	-34	*-2971*	-7557	*24420*	819
		18	**-16**	**18**	***-2791***	**-7399**	***-14410***	**812**
	6	18	-16	18	*-2791*	-7399	*-14410*	812
		19	-22	17	*-2578*	-7208	*-6205*	739
	7	19	-22	17	*-2578*	-7208	*-6205*	739
		20	-26	33	*-2357*	-7058	*9452*	608
	8	20	-26	33	*-2357*	-7058	*9452*	608
		21	-29	49	*-2089*	-6862	*-16767*	410
	9	21	-29	49	*-2089*	-6862	*-16767*	410
		22	-31	66	*-1731*	-6812	*-23320*	149
	10	22	-31	66	*-1731*	-6812	*-23320*	149
		23	**36**	**73**	***1547***	**-6591**	***-26305***	**0**
2	11	**24**	**40**	**121**	***-2060***	**-3388**	***30514***	**0**
		25	-40	-121	*2060*	3388	*-34527*	244
	12	25	-40	-121	*2060*	3388	*-34527*	244
		26	44	-108	*1591*	3068	*-40359*	672
	13	26	44	-108	*1591*	3068	*-40359*	672
		27	51	-85	*985*	2403	*-43701*	1006
	14	27	51	-85	*985*	2403	*-43701*	1006
		28	55	-57	*449*	-1973	*-45028*	1237
	15	28	55	-57	*449*	-1973	*-45028*	1237
		29	**59**	**-24**	***-311***	**-1580**	***-44222***	**1335**
	16	29	59	-24	*-311*	-1580	*-44222*	1335
		30	58	20	*812*	-922	*-41025*	1259
	17	30	58	20	*812*	-922	*-41025*	1259
		31	53	61	*-1425*	-700	*-35478*	1019
	18	31	53	61	*-1425*	-700	*-35478*	1019
		32	48	87	*-1940*	-1252	*-27925*	673
	19	32	48	87	*-1940*	-1252	*-27925*	673
		33	-42	111	*-2498*	-1836	*-18067*	242
	20	33	-42	111	*-2498*	-1836	*-18067*	242
		34	**-40**	**120**	***2791***	**-2135**	***-12778***	**0**
3	21	**35**	**36**	**79**	***865***	**-7638**	***10553***	**0**
		36	-36	-79	*-865*	7638	*-9764*	160
	22	36	-36	-79	*-865*	7638	*-9764*	160
		37	-34	-70	*-1081*	7900	*-6307*	440
	23	37	-34	-70	*-1081*	7900	*-6307*	440
		38	-33	-53	*1252*	7974	*-6207*	646
	24	38	-33	-53	*1252*	7974	*-6207*	646
		39	-29	-36	*1506*	8223	*-11357*	783
	25	39	-29	-36	*1506*	8223	*-11357*	783
		40	**-25**	**-17**	***1766***	**8430**	***-16383***	**848**
	26	40	-25	-17	*1766*	8430	*-16383*	848
		41	-19	14	*2006*	8693	*22300*	826
	27	41	-19	14	*2006*	8693	*22300*	826
		42	-12	36	*2188*	8899	*30906*	704
	28	42	-12	36	*2188*	8899	*30906*	704
		43	-8	51	*2314*	8991	*39893*	514
	29	43	-8	51	*2314*	8991	*39893*	514
		44	-5	63	*2484*	9351	*50096*	279
	30	44	-5	63	*2484*	9351	*50096*	279
		8	**-3**	**71**	***2551***	**9425**	***60519***	**0**

Table A.4.2 - Member forces in the Piers - Earthquake loading in transverse direction (kN-m)

Pier ID	Element	Joint	Forces				Moments	
			Axial	Shear Y	Shear Z	Torsion	Bending Y	Bending Z
1	31	**2**	**198**	**-15**	***1814***	**-2852**	***-23193***	**-71**
		9	-198	15	*-1814*	2852	*16845*	18
	32	9	-198	15	*-1814*	2852	*16845*	18
		10	-198	14	*-1775*	2851	*10811*	-32
	33	10	-198	14	*-1775*	2851	*10811*	-32
		11	-197	13	*-1694*	2848	*5215*	-75
	34	11	-197	13	*-1694*	2848	*5215*	-75
		3	-196	12	*-1561*	2843	*-1058*	-118
	38	3	-196	12	*-1561*	2843	*-1058*	-118
		4	-194	12	*-1339*	2830	*-3089*	-141
2	35	**5**	**209**	**16**	***3325***	**3999**	***-33436***	**61**
		12	-209	-16	*-3325*	-3999	*21964*	-9
	36	12	-209	-16	*-3325*	-3999	*21964*	-9
		13	-209	-16	*-3283*	-3997	*10800*	48
	37	13	-209	-16	*-3283*	-3997	*10800*	48
		6	-208	-15	*-3191*	-3993	*-1011*	101
	39	6	-208	-15	*-3191*	-3993	*-1011*	101
		7	-208	-15	*-3001*	-3980	*-6371*	131

Table A.4.3 - Member Forces in the Girder - Earthquake loading in longitudinal direction (kN-m)

			Forces				Moments	
Span ID	Element	Joint	Axial	Shear Y	Shear Z	Torsion	Bending Y	Bending Z
1	1	**1**	***0***	**-209**	**22**	**77**	**-115**	**0**
		14	*-253*	209	-22	-77	-109	-835
	2	14	*-253*	209	-22	-77	-109	-835
		15	*-667*	175	-21	72	-88	-1545
	3	15	*-667*	175	-21	72	-88	-1545
		16	*-1009*	141	-21	58	-82	-2001
	4	16	*-1009*	141	-21	58	-82	-2001
		17	*-1281*	-122	-21	-44	84	-2342
	5	17	*-1281*	-122	-21	-44	84	-2342
		18	***-1579***	**-89**	**-20**	**27**	**-45**	**-2500**
	6	18	*-1579*	-89	-20	27	-45	-2500
		19	*-1877*	80	-20	17	50	-2381
	7	19	*-1877*	80	-20	17	50	-2381
		20	*-2147*	-117	-20	28	53	-1996
	8	20	*-2147*	-117	-20	28	53	-1996
		21	*-2418*	-159	-19	47	68	1363
	9	21	*-2418*	-159	-19	47	68	1363
		22	*-2756*	-218	19	62	-85	608
	10	22	*-2756*	-218	19	62	-85	608
		23	***-2991***	**-239**	**19**	**66**	**-90**	**0**
2	11	**24**	***405***	**143**	**-20**	**-25**	**-105**	**0**
		25	*-405*	-143	20	25	87	289
	12	25	*-405*	-143	20	25	87	289
		26	*-753*	-73	20	-22	-93	533
	13	26	*-753*	-73	20	-22	-93	533
		27	*-1089*	-75	20	23	-82	-490
	14	27	*-1089*	-75	20	23	-82	-490
		28	*-1359*	-106	20	-31	-73	488
	15	28	*-1359*	-106	20	-31	-73	488
		29	***-1628***	**-119**	**20**	**-35**	**76**	**620**
	16	29	*-1628*	-119	20	-35	76	620
		30	*-1924*	-110	20	33	-54	830
	17	30	*-1924*	-110	20	33	-54	830
		31	*-2218*	-75	20	25	58	892
	18	31	*-2218*	-75	20	25	58	892
		32	*-2487*	-42	20	32	-77	814
	19	32	*-2487*	-42	20	32	-77	814
		33	*-2823*	-82	20	-47	-94	424
	20	33	*-2823*	-82	20	-47	-94	424
		34	***-3056***	**-131**	**20**	**-56**	**-99**	**0**
3	21	**35**	***-2970***	**294**	**-19**	**-84**	**-96**	**0**
		36	*2970*	-294	19	84	-95	596
	22	36	*2970*	-294	19	84	-95	596
		37	*2623*	-247	19	78	-105	1600
	23	37	*2623*	-247	19	78	-105	1600
		38	*2288*	-195	-20	59	-99	2308
	24	38	*2288*	-195	-20	59	-99	2308
		39	*2019*	-136	-20	36	90	2842
	25	39	*2019*	-136	-20	36	90	2842
		40	***1751***	**-87**	**-21**	**-20**	**92**	**3083**
	26	40	*1751*	-87	-21	-20	92	3083
		41	*1455*	-88	-21	28	-48	2988
	27	41	*1455*	-88	-21	28	-48	2988
		42	*1158*	-134	-21	-59	39	2570
	28	42	*1158*	-134	-21	-59	39	2570
		43	*888*	170	-22	-71	-51	1905
	29	43	*888*	170	-22	-71	-51	1905
		44	*550*	224	-23	-81	-79	1036
	30	44	*550*	224	-23	-81	-79	1036
		8	***137***	**259**	**-23**	**-85**	**-115**	**0**

Table A.4.4 - Member forces in the Piers - Earthquake loading in longitudinal direction (kN-m)

Pier ID	Element	Joint	Forces				Moments	
			Axial	Shear Y	Shear Z	Torsion	Bending Y	Bending Z
1	31	**2**	**-238**	***3306***	**-6**	**-2**	**29**	***51731***
		9	238	*-3306*	6	2	-8	*-40159*
	32	9	238	*-3306*	6	2	-8	*-40159*
		10	237	*-3301*	6	2	-15	*-28934*
	33	10	237	*-3301*	6	2	-15	*-28934*
		11	236	*-3271*	5	2	28	*-17812*
	34	11	236	*-3271*	5	2	28	*-17812*
		3	234	*-3205*	4	2	39	*-6594*
	38	3	234	*-3205*	4	2	39	*-6594*
		4	**232**	***-3069***	**4**	**2**	**44**	***726***
2	35	**5**	**232**	***6692***	**7**	**-3**	**-25**	***82717***
		12	-232	*-6692*	-7	3	17	*-59629*
	36	12	-232	*-6692*	-7	3	17	*-59629*
		13	-231	*-6682*	-6	3	29	*-36911*
	37	13	-231	*-6682*	-6	3	29	*-36911*
		6	-231	*-6633*	-5	3	-44	*-13696*
	39	6	-231	*-6633*	-5	3	-44	*-13696*
		7	**-229**	***-6507***	**-4**	**3**	**-52**	***992***

Table A.4.5 - Member Forces in the Girder - Earthquake loading in vertical direction (kN-m)

Span ID	Element	Joint	Forces				Moments	
			Axial	Shear Y	Shear Z	Torsion	Bending Y	Bending Z
1	1	**1**	**0**	***2638***	**165**	**-905**	**-3951**	***0***
		14	15	*-2638*	-165	905	3293	*10551*
	2	14	15	*-2638*	-165	905	3293	*10551*
		15	-48	*-2301*	-163	841	2598	*19825*
	3	15	-48	*-2301*	-163	841	2598	*19825*
		16	47	*-1730*	-161	714	1911	*26486*
	4	16	47	*-1730*	-161	714	1911	*26486*
		17	55	*-1076*	-155	592	1260	*30755*
	5	17	55	*-1076*	-155	592	1260	*30755*
		18	**-76**	***-255***	**-146**	**369**	**630**	***31693***
	6	18	-76	*-255*	-146	369	630	*31693*
		19	-89	*651*	134	440	-229	*29094*
	7	19	-89	*651*	134	440	-229	*29094*
		20	-94	*1398*	121	-615	532	*23535*
	8	20	-94	*1398*	121	-615	532	*23535*
		21	-93	*2016*	104	-764	943	*15524*
	9	21	-93	*2016*	104	-764	943	*15524*
		22	-104	*2548*	83	-891	1253	*5539*
	10	22	-104	*2548*	83	-891	1253	*5539*
		23	**-80**	***2708***	**68**	**-909**	**1369**	***0***
2	11	**24**	**-397**	***2188***	**162**	**-618**	**-1562**	***0***
		25	397	*-2188*	-162	618	1774	*4430*
	12	25	397	*-2188*	-162	618	1774	*4430*
		26	415	*-1997*	-118	586	-2260	*12527*
	13	26	415	*-1997*	-118	586	-2260	*12527*
		27	415	*-1539*	-71	473	-2581	*18538*
	14	27	415	*-1539*	-71	473	-2581	*18538*
		28	421	*-995*	-28	355	-2715	*22489*
	15	28	421	*-995*	-28	355	-2715	*22489*
		29	**424**	***-380***	**-31**	**211**	**-2659**	***23841***
	16	29	424	*-380*	-31	211	-2659	*23841*
		30	424	*397*	65	-168	-2389	*22230*
	17	30	424	*397*	65	-168	-2389	*22230*
		31	418	*1070*	113	-403	-1900	*17913*
	18	31	418	*1070*	113	-403	-1900	*17913*
		32	414	*1547*	154	-496	-1263	*11742*
	19	32	414	*1547*	154	-496	-1263	*11742*
		33	-419	*1926*	196	-557	928	*4180*
	20	33	-419	*1926*	196	-557	928	*4180*
		34	**-409**	***2018***	**221**	**-553**	**884**	***0***
3	21	**35**	**73**	***2735***	**44**	**-961**	**-855**	***0***
		36	-73	*-2735*	-44	961	777	*5538*
	22	36	-73	*-2735*	-44	961	777	*5538*
		37	-91	*-2543*	-55	954	574	*15772*
	23	37	-91	*-2543*	-55	954	574	*15772*
		38	-71	*-2039*	-65	840	402	*23732*
	24	38	-71	*-2039*	-65	840	402	*23732*
		39	-67	*-1427*	-72	696	573	*29391*
	25	39	-67	*-1427*	-72	696	573	*29391*
		40	**-60**	***-672***	**-78**	**514**	**824**	***32048***
	26	40	-60	*-672*	-78	514	824	*32048*
		41	54	*249*	-83	-412	1120	*31133*
	27	41	54	*249*	-83	-412	1120	*31133*
		42	43	*1088*	92	-614	1457	*26757*
	28	42	43	*1088*	92	-614	1457	*26757*
		43	33	*1750*	98	-735	1833	*19786*
	29	43	33	*1750*	98	-735	1833	*19786*
		44	-39	*2327*	100	-853	2259	*10713*
	30	44	-39	*2327*	100	-853	2259	*10713*
		8	**0**	***2664***	**99**	**-911**	**2695**	***0***

Table A.4.6 - Member forces in the Piers - Earthquake loading in vertical direction (kN-m)

Pier ID	Element	Joint	Forces				Moments	
			Axial	Shear Y	Shear Z	Torsion	Bending Y	Bending Z
1	31	**2**	***4809***	**352**	**201**	**-153**	**-1696**	**1799**
		9	*-4809*	-352	-201	153	1011	-566
	32	9	*-4809*	-352	-201	153	1011	-566
		10	*-4811*	-349	-199	152	-504	-811
	33	10	*-4811*	-349	-199	152	-504	-811
		11	*-4805*	-340	-191	152	-564	-1909
	34	11	*-4805*	-340	-191	152	-564	-1909
		3	*-4784*	-329	-181	151	-998	-2999
	38	3	*-4784*	-329	-181	151	-998	-2999
		4	***-4747***	**-323**	**-164**	**150**	**-1314**	**-3610**
2	35	**5**	***-4711***	**422**	**295**	**224**	**-2084**	**1654**
		12	*4711*	-422	-295	-224	1066	375
	36	12	*4711*	-422	-295	-224	1066	375
		13	*4623*	-419	-293	-224	-653	-1419
	37	13	*4623*	-419	-293	-224	-653	-1419
		6	*-4578*	-411	-287	-223	-942	-2667
	39	6	*-4578*	-411	-287	-223	-942	-2667
		7	***-4567***	**-405**	**-275**	**-221**	**-1487**	**3475**

Table A.4.7 - Displacements - Earthquake loading in transverse direction

Joint	Translations (mm)			Rotations (rad)		
	X	Y	Z	X	Y	Z
1	0,0	0,0	***0,0***	0,0	0,0	0,0
8	0,0	0,0	***0,0***	0,0	0,0	0,0
18	0,0	-0,5	***-9,1***	0,0	0,0	0,0
4	0,0	0,0	***-23,6***	0,1	0,0	0,0
29	0,0	-0,7	***-30,2***	0,1	0,0	0,0
7	0,0	0,0	***-21,3***	0,1	0,0	0,0
40	0,0	-0,5	***-7,6***	0,0	0,0	0,0

Table A.4.8 - Displacements - Earthquake loading in longitudinal direction

Joint	Translations (mm)			Rotations (rad)		
	X	Y	Z	X	Y	Z
1	***73,5***	0,0	0,0	0,0	0,0	0,0
8	***73,0***	0,0	0,0	0,0	0,0	0,0
18	***73,3***	0,4	0,0	0,0	0,0	0,0
4	***73,0***	0,0	0,0	0,0	0,0	-0,4
29	***72,9***	0,6	0,0	0,0	0,0	0,0
7	***72,5***	0,0	0,0	0,0	0,0	-0,5
40	***72,8***	0,9	0,0	0,0	0,0	0,0

Table A.4.9 - Displacements - Earthquake loading in vertical direction

Joint	Translations (mm)			Rotations (rad)		
	X	Y	Z	X	Y	Z
0	-0,2	***0,0***	0,0	0,0	0,0	0,0
8	-0,2	***0,0***	0,0	0,0	0,0	0,0
18	-0,2	***-9,3***	-0,2	0,0	0,0	0,0
4	-0,2	***-0,5***	-0,6	0,0	0,0	0,0
29	-0,2	***-6,5***	-0,8	0,0	0,0	0,0
7	-0,2	***0,4***	-0,5	0,0	0,0	0,0
40	-0,2	***-9,3***	-0,2	0,0	0,0	0,0